International Review of Financial Analysis 96 (2024) 103617

Contents lists available at ScienceDirect

International Review of Financial Analysis

journal homepage: www.elsevier.com/locate/irfa

Exploring asymmetries in cryptocurrency intraday returns and implied volatility: New evidence for high-frequency traders

Muhammad Mahmudul Karim [a], Mohamed Eskandar Shah [b], Abu Hanifa Md. Noman [a], Larisa Yarovaya [c,*]

[a] TIFIES Research Group And Southampton Malaysia Business School, University of Southampton Malaysia, 79100 Iskandar Puteri, Johor, Malaysia
[b] Hamad bin Khalifa University, Qatar Foundation, Qatar
[c] Centre for Digital Finance, Southampton Business School, University of Southampton, United Kingdom

ARTICLE INFO

JEL classifications:
C58
G11
G15

Keywords:
Return-volatility
Cryptocurrencies
Asymmetric
Quintile regression
Return frequencies

ABSTRACT

This paper aims to analyze the return-volatility relationship of Bitcoin and Ethereum across different return frequencies and all conditional quantiles of implied volatility, based on a unique 6.5 million observations. We employ the newly constructed Model-Free Implied Volatility (MFIV) of Bitcoin (BitVol) and Ethereum (EthVol) and use an asymmetric Quantile Regression Model (QRM) to capture the intraday asymmetric return-volatility relationship at different quantiles of the distribution of the dependent variable. Our findings show that the estimated coefficient using daily data is significant only at medium- to high-volatility regimes, while the estimated coefficients using high-frequency data are highly significant across all volatility regimes. Moreover, our results indicate that the asymmetry varies across frequencies and quantiles, with weak asymmetric effects at low quantiles and high frequencies, and strong asymmetric effects at high quantiles and low frequencies. This study provides new insight, especially for high-frequency traders.

1. Introduction

Cryptocurrency has emerged as a dynamic market, demonstrating significant market capitalization compared to traditional asset markets since its inception in 2009. The cryptocurrency markets have witnessed periods of explosive growth, such as in 2017 when the Bitcoin price reached $20,000 USD for the first time (Corbet et al., 2018). More recently, the decentralized finance (DeFi) bubble in 2020, fueled by the emergence of new and innovative crypto assets built on the Ethereum protocol, marked another period of rapid growth (Wang et al., 2022). As of November 2023, the number of actively traded cryptocurrencies has grown to 8843, with a combined market capitalization of US$1.45 trillion.[1] Bitcoin and Ethereum continue to maintain their positions as market leaders in the cryptocurrency space. While both cryptocurrencies operate on blockchain technology, their technological characteristics differ substantially. According to the classification provided by Corbet et al. (2019), Bitcoin can be categorized as a pure cryptocurrency with a primary focus on fund transfers, whereas Ethereum functions as a protocol, serving as a platform for the development of various decentralized finance (DeFi) assets.

We examine the asymmetric relationships between the return of Bitcoin and its implied volatility, as well as the return of Ethereum and its implied volatility, using high-frequency intraday data. Our study is motivated by recent findings reported by Karim et al. (2023), who investigated the efficacy of implied volatility as a robust estimator for short-term volatility in underlying assets. They employed newly constructed model-free implied volatility (MFIV) indices (BitVol and EthVol) for Bitcoin and Ethereum, along with asymmetric quantile regression and Non-linear ARDL approaches, to highlight significant differences in cryptocurrency volatility-return relationships compared to those reported for equity markets. Additionally, Kakinaka and Umeno (2022) analyzed the co-movements among 32 digital assets before and during the COVID-19 pandemic, noting an increase in the influential power of Ethereum over Bitcoin. Another noteworthy paper by Kakinaka and Umeno (2022) analyzed the asymmetric relationships among six cryptocurrencies using 5-min data, highlighting the significance of

* Corresponding author.
E-mail addresses: m.m.karim@soton.ac.uk (M.M. Karim), mrasid@hbku.edu.qa (M.E. Shah), AH.Alam@soton.ac.uk (A.H.Md. Noman), L.Yarovaya@soton.ac.uk (L. Yarovaya).

[1] Please see coinmarketcap.com for the most recent statistics.

https://doi.org/10.1016/j.irfa.2024.103617
Received 20 December 2023; Received in revised form 8 September 2024; Accepted 21 September 2024
Available online 24 September 2024

investment horizons in determining the reaction of cryptocurrency volatility to return shocks. According to Lahiani et al. (2021), due to information asymmetry and a lack of market regulation in the absence of a central regulatory authority, cryptocurrencies are more volatile than conventional assets, leading to greater risk and return for cryptocurrency investors. However, Yu et al. (2019) argued that market volatility makes the cryptocurrency market more efficient than the conventional assets market. Due to these unique characteristics, examining the return-volatility nexus of these two influential cryptocurrencies has become one of the most intriguing topics among scholars, policymakers, and investors.

Our study extends the work of Kakinaka and Umeno (2022) and Karim et al. (2023) by investigating the asymmetry of the return-volatility relationship of Bitcoin and Ethereum at different frequencies (1 m, 5 m, 10 m, 15 m, 60 m, and daily) and quantiles (i.e., low to high volatility regimes) using the MFIV of Bitcoin and Ethereum. In particular, our main objective is to explore the return-volatility relationship of these two major cryptocurrencies using high-frequency data, which allows us to uncover aspects of the relationship that cannot be identified with low-frequency data. Our choice is based on two primary factors. First, not only do Bitcoin and Ethereum account for over 60 % of the cryptocurrency market share, but they are also both highly traded and extremely liquid assets.

Second, and more importantly, options contracts are available for these two cryptocurrencies, enabling the measurement of their implied volatility. This is significant because option-implied volatility estimates the future realized volatility (RV) of the underlying assets over the life of the options (Badshah, 2013; Karim & Masih, 2021) and is often referred to as an "investor's fear gauge" (Whaley, 2000). We acknowledge that previous studies have analyzed a larger number of cryptocurrencies, such as Yarovaya and Zieba (2022) and Banerjee (2021), among others. However, in this paper, we focus our analysis specifically on Bitcoin and Ethereum, drawing from a substantial dataset comprising 6.5 million observations. This dataset includes high-frequency data ranging from minute-by-minute to daily intervals. Such a detailed examination provides valuable insights for various stakeholders in the cryptocurrency ecosystem, including high-frequency traders, hedge fund managers, and regulators.

For cryptocurrency investors, information on high-frequency intraday returns and implied volatility provides crucial insights into price movements and noise patterns across different timeframes and investment horizons. This helps in making more informed investment decisions and effectively hedging positions, particularly in volatile market conditions. Hedge fund managers can leverage this information to diversify their cryptocurrency portfolios and optimize trading strategies. Additionally, regulators and policymakers benefit from high-frequency returns and volatility data when assessing systemic risk and monitoring market stability, both in normal and crisis periods. This enables them to formulate and implement regulatory frameworks aimed at preventing market manipulation and safeguarding the stability of the cryptocurrency market.

This study contributes to the literature in several ways. First, we utilize the newly constructed model-free implied volatility (MFIV) measures for Bitcoin (BitVol) and Ethereum (EthVol). Unlike the standard Black-Scholes implied volatility (BSIV), which typically relies on options traded at the money (ATM), MFIV estimation incorporates a wide range of options across various moneyness levels. Consequently, MFIV offers a more accurate estimate of short-term predicted volatility compared to traditional BSIV, as it is built using the variance swap process. Furthermore, BitVol and EthVol are forward-looking volatility estimates (30-day implied volatility) based on the full range of option strikes (across all moneyness), providing the best indicator of Bitcoin and Ethereum's short-term projected volatility.

Second, building upon the works of Cheikh et al. (2020), Baur et al. (2018), and Karim et al. (2023), we investigate the intraday (i.e., 1, 5, 10, 15, and 60 min, and daily) asymmetric return-volatility relationship of cryptocurrencies (Bitcoin and Ethereum) using recently introduced implied volatility measures such as BitVol and EthVol. This study is one of the first attempts to explore asymmetric return-volatility relationships of cryptocurrencies using high-frequency return data and model-free implied volatility (MFIV).

Third, we utilize a dataset that is particularly unique and comprehensive, comprising 6.5 million observations gathered at various frequencies, including Model-Free Implied Volatility (MFIV) data obtained from the index provider. With the index's inception date set on 4th April 2020, this dataset spans a crucial period in the cryptocurrency market's history, coinciding with the onset of the COVID-19 pandemic. This timeframe is characterized by significant market turbulence and volatility, making it especially relevant for investigating the dynamics of cryptocurrency returns and implied volatility. By analyzing such a vast and diverse dataset, our study offers valuable insights into the behavior of cryptocurrency markets during this unprecedented period of global economic uncertainty.

Finally, in addition to Ordinary Least Squares (OLS) regression, we employ the Asymmetric Quantile Regression Model (QRM), a suitable method for capturing the asymmetric relationship between returns and volatility across different quantiles of the dependent variable's distribution (Badshah et al., 2016; Karim et al., 2022; Koenker, 2005). Our objective is to expand this analysis to encompass various volatility regimes, ranging from low to high volatility, recognizing that asymmetry, if present, may manifest differently across the conditional distribution of volatility and at different frequencies (1 m, 5 m, 10 m, 15 m, 60 m, and daily). Additionally, to enhance the robustness of our findings, we have employed wavelet coherence analysis, drawing on the methodologies used in Grinsted et al. (2004), Aguilera and Radetzki (2017), Pal and Mitra (2017), and Karim and Masih (2019). Wavelet coherence analysis offers several advantages for understanding the relationship between returns and volatility in financial time series data. Unlike traditional methods, wavelet coherence provides both time and frequency localization, allowing for the identification of how this relationship evolves over time at different frequencies.

Our findings show that the return-volatility relationship of cryptocurrency has different asymmetries across the different volatility regimes and trading frequencies, and those asymmetries seem to be more pronounced at extreme tails of the volatility distribution. To illustrate, it was observed that, first, the return-volatility relationship is more pronounced at daily data interval (i.e., low-frequency data) than the intraday data interval (i.e., high-frequency data). Second, the asymmetry of return-volatility was high based on lower-frequency data (i.e., daily data); whereas, using high-frequency data (i.e., 1-min data), the asymmetry of return-volatility was less visible. In particular, the use of low-frequency data (i.e., daily data) resulted in better visibility of asymmetry at medium to uppermost quantiles of the volatility distribution, while the use of high-frequency data (i.e., 1-min data) generated more visible asymmetry at lower quantiles of the volatility distributions. Third, our results indicate that the response to negative (positive) returns is a monotonically decreasing (increasing) function of the return horizons. Fourth, the absolute values of the estimated coefficients were increasing as we move from the highest frequency of the data to its lowest frequency (i.e.: daily >60 m $>$ 15 m $>$ 10 m $>$ 5 m $>$ 1 m). Furthermore, the absolute values of the estimated coefficients were also increasing as we move from the lowest quantiles ($q = 0.05$) to the highest quantile ($q = 0.95$) of the volatility distributions. Unlike previous studies, our findings are unique and show the need to differentiate high-frequency data from daily ones.

The major similarity in the estimated results of intraday and daily data intervals is that, during the medium to high volatility regimes, both positive and negative return shocks were positively associated with the changes in volatility. This also supports the finding of Baur et al. (2018) and Karim et al. (2023) based on the daily data. Furthermore, using the daily data, a positive return shock tends to create a greater response to cryptocurrency volatility compared to the volatility response to a

negative return shock. Also, good news was observed to generate more impact on cryptocurrency volatility, compared to bad news. This positive asymmetric (inverted asymmetric) reaction is attributed to the noise trading activity, as shown by Karim et al. (2023), Baur et al. (2018) and Cheikh et al. (2020). Conventional wisdom says: "volatility increases following a negative return shock." However, increasing the volatility of the cryptocurrencies following a positive return shock tends to disrupt the conventional understanding of the return-volatility relationship. Since there is no proper theoretical model for the valuation of the cryptocurrencies' prices, any positive price movement tends to elevate the speculative behavior of the market participants regarding the prospects of the cryptocurrencies. Hence, FOMO seems to play a crucial role in cryptocurrencies' prices Karim et al. (2023).

The rest of this paper is set out as follows: Section 2 discusses the background literature; Section 3 presents data and methodology. Section 4 discusses the findings, while Section 5 concludes our paper.

2. Literature review

The return-volatility relationship has been extensively studied in traditional markets, such as common stocks and bonds (see Badshah et al., 2016, for an excellent literature review). Empirical evidence from this literature has consistently confirmed an asymmetric (mostly negative) return-volatility relationship, commonly explained by two traditional theories: the leverage effect (Black, 1976; Christie, 1982) and the volatility feedback effect (Bekaaert & Wu, 2000; Campbell & Hentschel, 1992; French et al., 1987).

The leverage effect, also known as the 'asymmetric volatility effect,' posits that innovations in negative (positive) stock returns cause a decrease (increase) in stock value, leading to financial leverage and increased risk for stockholders, ultimately increasing stock volatility. Conversely, the volatility feedback hypothesis suggests that market prices stocks for volatility, and positive innovations in volatility increase the required rate of return, leading to a decrease in stock price, and vice versa.

Cryptocurrencies, however, differ from common stocks. They lack underlying assets, with their value mainly derived from the prospects of underlying technology, regulatory acceptance, store of value, and their utilization as a medium of exchange. Understanding the return-volatility relationship for cryptocurrencies is crucial to determine whether traditional theories apply or if new patterns are emerging. Recent studies on the cryptocurrency market have indicated herding behaviors rather than traditional leverage and volatility feedback effects due to the absence of a capital structure and the presence of safe-haven properties (Ballis & Drakos, 2020; Bouri et al., 2017; Da Gama Silva et al., 2019; Kakinaka & Umeno, 2022; Poyser, 2018; Yarovaya et al., 2020). Baur et al. (2018) argue that the cryptocurrency price is mainly driven by the fear-of-missing-out (FOMO) effect arising from the action of uninformed noise traders. Studies by Badshah et al. (2016) and Bouri et al. (2019), utilizing behavioral finance theory, provide strong evidence of an asymmetric return-volatility relationship.

Analyzing the return-volatility relationship through three behavioral finance theories — representation bias, effect bias, and extrapolation bias — sheds light on Tversky and Kahneman's (1974) representational bias. Investors evaluate investments based on their risk-return characteristics, favoring high-yielding and low-risk investments. The effect bias of Kahneman and Tversky (1979) explains the negative or positive asymmetric return and market volatility. Present emotional states, such as fear or greed, have an immediate effect on investors, perceiving any price decline as a sign of greater market volatility or risk, and vice versa. Shefrin's (2008) extrapolation bias suggests that investors extrapolate knowledge from past events to determine future action plans.

In addition to deviating from traditional leverage and volatility feedback effects, empirical results on bitcoin return volatility align more with behavioral theories. According to Bouri et al. (2017), Cheikh et al. (2020), Baur and Dimpfl (2018), Kakinaka and Umeno (2022), and Karim et al. (2023), inverted or positive asymmetric return volatility dominates negative asymmetric return volatility in the cryptocurrency market due to FOMO and the noise trading activity of uninformed investors. Specifically, Kakinaka and Umeno (2022) contribute by examining the scale-dependent structure of the asymmetric volatility effect in six representative cryptocurrencies: Bitcoin, Ethereum, Ripple, Litecoin, Monero, and Dash. Their dynamical approach, employing DFA-based fractal regression analysis, reveals that the asymmetric volatility phenomenon varies by scale and cryptocurrency, with a time-varying structure. Notably, minor currencies exhibit an "inverse" asymmetric volatility effect at relatively large scales, deviating from traditional equity markets.

Baranerjee et al. (2022) shift focus to the influence of COVID-19 news sentiment on cryptocurrency returns. Utilizing a nonlinear technique of transfer entropy, the study investigates the relationship between the top 30 cryptocurrencies by market capitalization and COVID-19 news sentiment. Surprisingly, the nexus is unidirectional, with COVID-19 news sentiment influencing cryptocurrency returns. This departure from past findings underscores the dynamic nature of cryptocurrency market dynamics under highly stressful conditions. Gkillas et al. (2022) contribute with a novel asymmetric jump model designed to model interactions in discontinuous movements in asset prices, particularly in cryptocurrency markets characterized by jump behavior and high volatility levels. Their study assesses the impact of various types of jumps on the discontinuity component of realized volatility across different cryptocurrencies, revealing significant asymmetric effects between small and large jumps and between downside and upside jumps. Co-jumping behavior is also identified, adding depth to the understanding of cryptocurrency market dynamics.

Li (2020) claims that information asymmetry impedes market efficiency and increases the mispricing of assets. In the cryptocurrency market, information asymmetry leads to an asymmetric return volatility, if positive and negative news affects the return volatility differently. Wan Jamarul Imran et al. (2021) observed that asymmetric information is associated with greater volatility in cryptocurrencies, particularly, Bitcoins and Ethereum, as investors react to the uncertain information, considering cryptocurrencies as speculative assets (Baek & Elbeck, 2015; Selgin, 2015). Several studies examined the informational efficiency of Bitcoin. First, Urquhart (2016) observed an inefficiency of the Bitcoin market, however, the author claimed the market illustrates a transitory phase to gain efficiency as the market matures. Later Nadarajah and Chu (2017) extended the hypothesis of Urquhart (2016) adding an odd integer power to the returns of Bitcoin and observed that Bitcoin returns are market efficient. Subsequently, Bariviera (2017) and Tiwari et al. (2018) also observed the Bitcoin markets are informationally efficient. In a related study, analyzing 456 cryptocurrencies, Wei (2018) observed that high liquidity contributes to diminishing return predictability and promoting market efficiency of cryptocurrencies.

Cross et al. (2021) analyzed the relationship in four major cryptocurrencies—Bitcoin, Ethereum, Litecoin, and Ripple—during the 2017–18 cryptocurrency bubble. Using an asset pricing model, they found a risk premium effect in Litecoin and Ripple during the 2017 boom. Adverse news significantly contributed to the 2018 cryptocurrency crash across all four cryptocurrencies. Furthermore, incorporating stochastic volatility and heavy-tailed distribution improves return and volatility forecasts, suggesting cryptocurrency markets were not weak-form efficient during this period.

Salisu and Ogbonna (2022) utilize hourly cryptocurrency data alongside daily news indicators, employing the GARCH MIDAS framework to handle differing data frequencies. They found that pandemic-related news amplifies cryptocurrency return volatilities relative to pre-pandemic periods. Furthermore, they showed that the predictive model, incorporating news effects, surpasses the benchmark (historical average) model in predicting return volatility.

In terms of research methodology, previous investigations have predominantly leaned towards the adoption of GARCH family models,

including the Component GARCH model (Katsiampa, 2017), Smooth Transition GARCH model (Cheikh et al., 2020), Threshold GARCH (Baur & Dimpfl, 2018; Cheikh et al., 2020), Exponential GARCH (Bouri et al., 2018; Cheikh et al., 2020), GJR GARCH (Bouri et al., 2018), and Threshold GJR GARCH (Cheikh et al., 2020). However, studying asymmetric return-volatility phenomena in the cryptocurrency realm using GARCH models faces challenges, given the market's exposure to substantial shocks leading to drastic price movements (Cheikh et al., 2020; Charles & Darné, 2019; Trucíos, 2019; Chaim & Laurini, 2018). Additionally, certain studies have utilized market-based (model-free) volatility estimation, such as realized volatility (Kakinaka & Umeno, 2022), and, notably, Implied Volatility (IV) estimation through Black-Scholes models. However, due to drawbacks associated with Black-Scholes Implied Volatility (BSIV), the Model-Free Implied Volatility (MFIV) based on the variance swap methodology has garnered increased attention (Karim et al., 2023). Empirical studies have demonstrated the superiority of MFIV, encompassing information on both past and expected volatility, and being estimated using a full range of option strikes (Karim et al., 2022).

3. Data & methodologies

We collected the daily and intraday data of Bitcoin and Ethereum volatility indices (BitVol and EthVol) from the T3 index provider. We then constructed datasets at different frequencies from the master dataset (i.e., 1, 5, 10, 15, and 60 min, and daily), spanning from the index inception date on April 4, 2020, to August 17, 2022. Following the same time and frequency, we have also collected the intraday data of BITUSD and ETHUSD from the CryptoDataDownload[2] website. The intraday high-frequency data of several cryptocurrencies traded globally were stored in different exchange houses. Finally, we have a total of almost 6.5 million observations for the analysis.

The literature offers valuable insights into handling noise in high-frequency data. Voev and Lunde (2007) address the impact of non-synchronicity and market microstructure noise on realized covariance estimators, proposing a subsampling version to enhance efficiency. Bibinger and Winkelmann (2015) contribute by establishing estimation methods for co-jumps in multivariate high-frequency data, employing a locally adaptive spectral approach and thresholding to disentangle co-jumps from the continuous part. Aït-Sahalia and Xiu (2019) develop tests to assess the suitability of high-frequency data for volatility estimation, based on the Hausman principle, offering a robustness versus efficiency trade-off. These approaches collectively provide practical tools for researchers and practitioners to navigate and mitigate the challenges posed by noise in high-frequency financial data.

Following Badshah et al. (2016), Karim et al. (2022) and Karim et al. (2023), we calculated the daily percentage of continuously compounded returns (denoted by *r_BTC* and *r_ETH* in Table 1) of the Bitcoin (BTC) and Ethereum (ETH) for all the sample frequencies using the formula (Eq. (1)) below:

$$100 \times (log(P_t) - log(P_{t-1})) \tag{1}$$

And, the percentage changes of the BitVol and EthVol (denoted by Δ*BitVol* and Δ*EthVol* in Table 1) for all the given frequencies of sample data were calculated as follows (Eq. (2)):

$$100 \times \left(\frac{MFIV_t - MFIV_{t-1}}{MFIV_{t-1}}\right) \tag{2}$$

The summary statistics of the sample data are reported in Table 1. Specifically, Table 1 reports a total of 6 data sets' (i.e., 1 m, 5 m, 10 m, 15 m, 60 m, and daily) summary statistics, unit roots and normality tests for the percentage changes of BitVol, EthVol, Bitcoin, and Ethereum. The results indicated that the mean return of Ethereum is comparatively higher than that of Bitcoin during our sample periods. The mean of the volatility changes, denoted by Δ*EVOL* and Δ*BVOL*, were almost the same but slightly higher for Ethereum. The test for skewness and kurtosis showed that the Bitcoin return is negatively skewed, Ethereum returns are positively skewed, and all the volatility indices' returns are positively skewed. Moreover, all the variables exhibited the leptokurtic, picked-curve (positive kurtosis) distribution. As a result, the Jarque-Bera statistics also reject the normality for each of the variables mentioned in Table 1. The last 2nd row of Table 1 shows the unit-roots test (using Augmented Dickey-Fuller and Phillips-Perron tests), and the results from both tests indicated that all four variables are stationary (reject the null hypothesis of non-stationary at 1 % level). However, all the variables were non-stationary in their level form, but stationary after taking first difference.

3.1. Quantile regression model

In addition to the OLS, this study applies the QRM proposed by by Koenker and Bassett Jr (1978), later on, reviewed and revised by Buchinsky (1998); Koenker and Hallock (2001); and Koenker (2005). The advantage of applying quantile regression is can provide a better understanding of the relationship between the variables outside the mean of the data. Moreover, it helps to understand the findings in the absence of normal distribution and the presence of a non-linear relationship. Thus, this method provides greater flexibility in comparison with other regression methods to identify heterogeneous relationships at different parts of the distribution of the outcome variable (Karim et al., 2022).

We define $\Delta MFIV_{it}$ (using Eq. (2)) as the percentage change in volatility and R_{it} (using Eq. (1)) as the daily percentage continuously compounded return of cryptocurrency, where $i = 1, 5, 10, 15, 60$-min and daily data frequencies. For positive returns (R_{it}^{+}) and negative returns (R_{it}^{-}), R_{it} was decomposed into two parts (Eq. (3)):

$$R_{it}^{+} = \begin{cases} R_{it} \text{ if } R_{it} > 0 \\ 0 \text{ if } R_{it} < 0 \end{cases} \text{ and } R_{it}^{-} = \begin{cases} R_{it} \text{ if } R_{it} < 0 \\ 0 \text{ if } R_{it} > 0 \end{cases} \tag{3}$$

Then, for the asymmetric relation, the standard mean-regression model (OLS) was developed as follows:

$$\Delta MFIV_{it} = \alpha_i + \sum_{L=1}^{3} \beta_{i\,L} \Delta MFIV_{it-L} + \sum_{L=0}^{3} \gamma_{i\,L} R_{it-L}^{+} + \sum_{L=0}^{3} \delta_{i\,L} R_{it-L}^{-} + u_{it} \tag{4}$$

Moreover, to examine the asymmetric relation at different quantiles, the following form of the equation was used for the asymmetric quantile regression (Eq. (5)):

$$\Delta MFIV_{it} = \alpha_i^{(q)} + \sum_{L=1}^{3} \beta_{i\,L}^{(q)} \Delta MFIV_{it-L} + \sum_{L=0}^{3} \gamma_{i\,L}^{(q)} R_{it-L}^{+} + \sum_{L=0}^{3} \delta_{i\,L}^{(q)} R_{it-L}^{-} + u_{it} \tag{5}$$

Here, $\alpha_i^{(q)}$ is the intercept of respective quantile (q) and frequencies (i), $\beta_{i\,L}^{(q)}$ is the coefficient of lagged $\Delta MFIV$ at respective quantile (q) and frequencies (i), where the lagged L = 1–3. The coefficients $\gamma_{i\,L}^{(q)}$ and $\delta_{i\,L}^{(q)}$ represent the impact of positive and negative returns of cryptocurrency at different quantiles (q) and frequencies (i), where the lagged L = 0–3 for both positive and negative returns. The error term u_{it} is assumed to be independent and derived from the error distribution of $\varnothing_q u_t$ with zero mean at the q^{th} quantile.

3.2. Wavelet coherence

For robustness cheking, building upon the research conducted by Aguilera and Radetzki (2017), Grinsted et al. (2004), Karim and Masih (2019), and Pal and Mitra (2017), our analysis employ wavelet coherence within the framework of a continuous wavelet transform. In this

[2] https://www.cryptodatadownload.com

Table 1
Summary statistics.

	1 m		5 m		10 m		15 m		60 m		Daily	
	ΔBitVol	*r_BTC*	*ΔBitVol*	*r_BTC*	*ΔBitVol*	*r_BTC*	*ΔBitVol*	*r_BTC*	*ΔBitVol*	*r_BTC*	*ΔBitVol*	*r_BTC*
Mean	0.0000547	0.0001012	0.0003163	0.0005056	0.0005707	0.0010109	0.0010496	0.0015169	0.0041062	0.0060721	0.092201	0.1472351
Median	0	0	0	0	0	0.0000987	0	0.0012779	−0.0213634	0.005702	−0.2203732	0.1172001
Max	27.72516	13.35119	56.61863	10.05352	31.65199	10.05352	58.97332	10.27359	28.1193	13.91214	26.94717	18.28581
Min	−24.59131	−11.35739	−19.77166	−11.80129	−19.89662	−14.77859	−32.66593	−10.94924	−20.75389	−9.614048	−18.65483	−17.50159
SD	0.1168193	0.115879	0.28353	0.2549398	0.3773989	0.3512784	0.5099919	0.4279409	0.9993574	0.8134587	4.944762	3.727895
Skewness	6.877104	0.9022726	35.6714	−0.5429257	6.023977	−0.7068409	18.59184	0.1347518	2.772519	0.0201255	1.056999	−0.1074517
Kurtosis	6859.366	414.5362	7360.448	94.23499	759.3149	74.75113	2626.44	36.25388	105.4593	18.27369	7.643496	5.534436
Jarque-Bera	2,400,000,000,000	8,500,000,000	540,000,000,000	84,000,000	2,900,000,000	26,000,000	23,000,000,000	3,700,000	8,800,000	200,000	915	228
P Value	0	0	0	0	0	0	0	0	0	0	0	0
ADF	−1041.936***	−1117.023***	−490.035***	−521.462***	−326.034***	−361.454***	−283.417***	−295.220***	−127.12***	−143.194***	−32.458 ***	−29.848 ***
PP	−1044.196***	−1120.421***	−491.857***	−522.966***	−329.289***	−362.297***	−284.046***	−295.908***	−126.642	−143.35***	−32.585***	−29.83***
WN	4550.3276***	3420.88***	549.6263***	1174.99***	1150.82***	434.179***	431.19***	338.35***	407.55	113.55***	73.88***	41.29***
Number Obs	1,204,723	1,204,723	240,938	240,938	120,489	120,489	80,334	80,334	20,091	20,091	845	845
	ΔEthVol	*r_ETH*	*ΔEthVol*	*r_ETH*	*ΔEthVol*	*r_ETH*	*ΔEthVol*	*r_ETH*	*ΔEthVol*	*r_ETH*	*ΔEthVol*	*r_ETH*
Mean	0.0000819	0.0002042	0.0004429	0.0010211	0.0008834	0.0020406	0.0014061	0.0030606	0.0060571	0.0122377	0.1664901	0.2946186
Median	0	0	0	0	0	0	0	0.0024079	−0.017599	0.0127809	−0.2423698	0.3992934
Max	20.31718	20.03371	29.91869	19.86074	20.19346	19.86074	33.46452	20.11264	36.80464	17.70892	67.1326	23.99775
Min	−18.1694	−11.11991	−13.61583	−13.47176	−13.53829	−15.63073	−13.53829	−15.96822	−14.81828	−12.54585	−24.05283	−30.37351
SD	0.1221597	0.1503149	0.2874478	0.3274827	0.4043856	0.4527971	0.5151299	0.5514652	1.070376	1.057075	5.85922	5.027502
Skewness	5.070796	1.883362	11.95121	0.4142548	5.303099	0.0408787	9.27665	0.3622077	4.194788	−0.0782881	2.612327	−0.2799596
Kurtosis	2059.763	451.7695	1178.937	117.0675	289.0201	76.68094	557.1394	50.10835	126.7176	15.5716	26.32073	6.243577
Jarque-Bera	210,000,000,000	10,000,000,000	6,800,000,000	96,000,000	410,000,000	27,000,000	1,000,000,000	7,400,000	13,000,000	130,000	20,000	379
P Value	0	0	0	0	0	0	0	0	0	0	0	0
ADF	−1044.64***	−1112.90***	−333.78 ***	−363.94 ***	−324.44***	−359.56***	−267.55***	−292.77***	−128.2 ***	−140.98***	−32.289***	−30.218***
PP	−1048.41***	−1116.19***	−480.94***	−516.36***	−327.52***	−360.03***	−269.39***	−293.28***	−128.4***	−141.0***	−32.41***	−30.19***
WN	5195.60***	2578.89***	836.36***	952.95***	906.65***	371.05***	500.29***	246.51***	348.92***	147.47***	69.40***	46.73***
Number Obs	1,199,434	1,199,434	118,137	118,137	119,923	119,923	79,957	79,957	19,989	19,989	840	840

Note: Table 1 presents the descriptive statistics of the return of Bitcoin, Ethereum, BITVOL and ETHVOL. *r_BTC* and *r_ETH* are the percentage continuous compounding return of Bitcoin and Ethereum. Δ*BitVol* and Δ*EthVol* are the percentage return of the ETHVOL and BITVOL. ADF (Augmented Dickey-Fuller) and PP (Phillips–Perron test) are the unit-root tests.). Portmanteau test is the white noise test. Jarque-Bera was used for the normality test. The rejection of the null hypothesis at 1 %, 5 % and 10 % levels were denoted by ***, ** and *, respectively.

Table 2
Testing the Changes of Bitcoin Volatility Across the Quantiles at 1-Minute Data Frequency.

Quantile	$\Delta BVOL_{t-1}$	$\Delta BVOL_{t-2}$	$\Delta BVOL_{t-3}$	R_t^+	R_{t-1}^+	R_{t-2}^+	R_{t-3}^+	R_t^-	R_{t-1}^-	R_{t-2}^-	R_{t-3}^-	Intercept	R^2
0.05	0.0113***	0.0274***	0.0188***	−0.149***	−0.813***	−0.255***	−0.112***	0.108***	0.253***	0.106***	0.0838***	−0.0347***	0.0778
	(6.17)	(15.05)	(10.73)	(−49.76)	(−269.50)	(−83.62)	(−37.32)	(35.50)	(81.84)	(33.75)	(26.78)	(−121.37)	
0.1	−0.00265**	0.0143***	0.0122***	−0.101***	−0.716***	−0.201***	−0.0853***	0.0740***	0.191***	0.0491***	0.0489***	−0.0163***	0.0782
	(−2.65)	(14.28)	(12.66)	(−61.24)	(−432.80)	(−120.58)	(−51.84)	(44.35)	(112.51)	(28.42)	(28.51)	(−104.16)	
0.15	−0.00981***	0.00697***	0.0101***	−0.0712***	−0.630***	−0.163***	−0.0668***	0.0544***	0.141***	0.0165***	0.0285***	−0.0103***	0.0852
	(−13.61)	(9.70)	(14.65)	(−60.24)	(−529.79)	(−135.97)	(−56.46)	(45.31)	(115.45)	(13.27)	(23.09)	(−91.09)	
0.2	−0.0131***	0.00354***	0.00844***	−0.0516***	−0.553***	−0.138***	−0.0527***	0.0413***	0.0936***	−0.00306**	0.0171***	−0.00717***	0.0972
	(−21.09)	(5.73)	(14.19)	(−50.68)	(−539.73)	(−133.03)	(−51.75)	(39.97)	(89.07)	(−2.86)	(16.12)	(−73.87)	
0.25	−0.0181***	0.000545	0.00718***	−0.0455***	−0.490***	−0.124***	−0.0491***	0.0359***	0.0534***	−0.0205***	0.0108***	−0.00366***	0.0809
	(−30.32)	(0.92)	(12.54)	(−46.47)	(−497.53)	(−124.64)	(−50.05)	(36.10)	(52.87)	(−19.96)	(10.59)	(−39.23)	
Median	−0.0176***	−0.000746	0.00398***	−0.00477***	−0.191***	−0.0582***	−0.0117***	−0.00333***	−0.192***	−0.0677***	−0.0164***	0.0000786	0.0511
	(−37.81)	(−1.61)	(8.93)	(−6.25)	(−248.55)	(−74.99)	(−15.35)	(−4.30)	(−243.25)	(−84.49)	(−20.55)	(1.08)	
0.75	−0.0130***	0.00455***	0.00799***	0.0360***	0.0523***	−0.0119***	0.0123***	−0.0363***	−0.483***	−0.126***	−0.0486***	0.00506***	0.0756
	(−23.08)	(8.11)	(14.81)	(39.01)	(56.28)	(−12.65)	(13.35)	(−38.70)	(−506.57)	(−129.91)	(−50.35)	(57.44)	
0.8	−0.00801***	0.00683***	0.00887***	0.0464***	0.0952***	0.00570***	0.0182***	−0.0457***	−0.552***	−0.144***	−0.0542***	0.00733***	0.0983
	(−13.36)	(11.43)	(15.45)	(47.25)	(96.27)	(5.70)	(18.54)	(−45.77)	(−544.46)	(−139.75)	(−52.77)	(78.20)	
0.85	−0.00255***	0.0109***	0.0106***	0.0640***	0.148***	0.0264***	0.0297***	−0.0638***	−0.636***	−0.172***	−0.0688***	0.00949***	0.1506
	(−3.67)	(15.84)	(16.02)	(56.34)	(129.18)	(22.83)	(26.08)	(−55.25)	(−541.65)	(−144.38)	(−57.95)	(87.57)	
0.9	0.00598***	0.0186***	0.0146***	0.0919***	0.208***	0.0639***	0.0538***	−0.0931***	−0.734***	−0.219***	−0.0877***	0.0131***	0.1812
	(6.37)	(19.85)	(16.28)	(59.70)	(134.08)	(40.84)	(34.88)	(−59.57)	(−461.95)	(−135.23)	(−54.53)	(89.10)	
0.95	0.0227***	0.0359***	0.0268***	0.148***	0.300***	0.146***	0.105***	−0.152***	−0.876***	−0.292***	−0.120***	0.0238***	0.2256
	(12.83)	(20.39)	(15.81)	(51.20)	(102.82)	(49.48)	(36.03)	(−51.51)	(−292.99)	(−95.77)	(−39.58)	(86.29)	
OLS	0.0244	0.0206	−0.0155	0.0391	−0.267***	−0.0666***	−0.0220	−0.0413**	−0.293***	−0.107***	−0.0308	−0.00512***	0.13738
	(0.88)	(0.95)	(−0.56)	(1.69)	(−6.27)	(−3.77)	(−1.89)	(−2.87)	(−14.36)	(−5.30)	(−1.30)	(−3.39)	

Notes. We provide findings from the lower to upper (i.e., 0.05 to 0.95) quantile regressions and the OLS regression of the changes of *BITVOL* on the set of independent variables. $\Delta BVOL_{t-1}$, $\Delta BVOL_{t-2}$ and $\Delta BVOL_{t-3}$ represent the lags of the changes of *BITVOL*. The positive return of Bitcoin is denoted by R_t^+, while the negative return of this cryptocurrency is denoted by R_t^-. Note that R_{t-1}^+, R_{t-2}^+ and R_{t-3}^+ are the lags of the positive returns. R_{t-1}^-, R_{t-2}^- and R_{t-3}^- are the lags of the negative returns. The significance levels at 1 %, 5 % and 10 % are denoted by ***, ** and *, respectively. The t-statistics are given in parentheses.

Table 3
Testing the Changes of Bitcoin Volatility Across the Quantiles at Daily Data Frequency.

Quantile	$\Delta BVOL_{t-1}$	$\Delta BVOL_{t-2}$	$\Delta BVOL_{t-3}$	R_t^+	R_{t-1}^+	R_{t-2}^+	R_{t-3}^+	R_t^-	R_{t-1}^-	R_{t-2}^-	R_{t-3}^-	Intercept	R^2
0.05	−0.146	−0.167	−0.0369	−0.216	−0.146	−0.317	−0.311	−0.427*	0.149	0.172	0.384	−4.982***	0.1554
	(−1.64)	(−1.87)	(−0.42)	(−1.17)	(−0.78)	(−1.69)	(−1.67)	(−2.27)	(0.73)	(0.83)	(1.87)	(−5.42)	
0.1	−0.0795	−0.123	−0.0810	−0.192	−0.194	−0.201	−0.0363	−0.492***	0.240	0.0196	0.108	−4.172***	0.1044
	(−1.15)	(−1.77)	(−1.19)	(−1.33)	(−1.33)	(−1.38)	(−0.25)	(−3.37)	(1.51)	(0.12)	(0.68)	(−5.84)	
0.15	−0.0707	−0.129*	−0.0629	−0.138	−0.203	−0.0850	0.144	−0.531***	0.377**	−0.00112	0.163	−3.285***	0.0737
	(−1.36)	(−2.47)	(−1.22)	(−1.27)	(−1.85)	(−0.78)	(1.32)	(−4.84)	(3.14)	(−0.01)	(1.36)	(−6.12)	
0.2	−0.0792	−0.116**	−0.0382	−0.103	−0.214*	−0.122	0.0942	−0.557***	0.344***	−0.0577	0.0895	−2.716***	0.0726
	(−1.81)	(−2.64)	(−0.88)	(−1.14)	(−2.32)	(−1.32)	(1.03)	(−6.04)	(3.42)	(−0.57)	(0.89)	(−6.02)	
0.25	−0.0961*	−0.110**	−0.00660	−0.0768	−0.242**	−0.0317	0.0281	−0.508***	0.327***	−0.0704	0.124	−2.104***	0.0812
	(−2.36)	(−2.69)	(−0.16)	(−0.91)	(−2.82)	(−0.37)	(0.33)	(−5.91)	(3.47)	(−0.74)	(1.32)	(−5.00)	
Median	−0.0560	−0.0879**	−0.0578	0.168*	−0.206**	−0.0767	0.0322	−0.738***	0.346***	−0.0284	−0.0244	−0.515	0.0893
	(−1.78)	(−2.79)	(−1.86)	(2.57)	(−3.11)	(−1.16)	(0.49)	(−11.15)	(4.78)	(−0.39)	(−0.34)	(−1.59)	
0.75	−0.00991	−0.00868	−0.0961*	0.597***	−0.164	−0.0331	0.121	−1.103***	0.342**	−0.178	−0.154	0.509	0.1464
	(−0.20)	(−0.18)	(−1.99)	(5.86)	(−1.59)	(−0.32)	(1.18)	(−10.69)	(3.03)	(−1.57)	(−1.36)	(1.01)	
0.8	−0.0264	−0.00200	−0.0913*	0.767***	−0.173	0.0112	0.0515	−1.255***	0.361***	−0.266**	−0.150	0.716	0.1759
	(−0.61)	(−0.05)	(−2.14)	(8.53)	(−1.90)	(0.12)	(0.57)	(−13.80)	(3.63)	(−2.66)	(−1.50)	(1.61)	
0.85	0.0408	0.0379	−0.0705	0.841***	−0.0810	0.0881	0.0145	−1.332***	0.417***	−0.265*	−0.0947	1.201*	0.212
	(0.79)	(0.73)	(−1.38)	(7.82)	(−0.74)	(0.81)	(0.13)	(−12.23)	(3.50)	(−2.21)	(−0.79)	(2.25)	
0.9	0.0335	0.0654	−0.0114	1.003***	−0.0481	0.0524	0.0982	−1.605***	0.362	−0.206	−0.131	1.555	0.2722
	(0.40)	(0.78)	(−0.14)	(5.77)	(−0.27)	(0.30)	(0.56)	(−9.12)	(1.88)	(−1.06)	(−0.68)	(1.80)	
0.95	0.107	0.111	−0.0240	1.953***	0.0223	0.0328	0.00841	−1.863***	0.490**	−0.274	−0.373*	1.683*	0.3486
	(1.30)	(1.34)	(−0.30)	(11.42)	(0.13)	(0.19)	(0.05)	(−10.77)	(2.59)	(−1.44)	(−1.97)	(1.99)	
OLS	−0.0557	−0.0556	−0.0552	0.376**	−0.0820	−0.0570	0.0841	−0.950***	0.345***	−0.0181	−0.0121	−1.145**	0.2370
	(−1.33)	(−1.28)	(−1.39)	(2.81)	(−0.97)	(−0.78)	(1.12)	(−9.13)	(4.34)	(−0.18)	(−0.11)	(−3.19)	

Notes. We provide findings from the lower to upper (i.e., 0.05 to 0.95) quantile regressions and the OLS regression of the changes of *BITVOL* on the set of independent variables. $\Delta BVOL_{t-1}$, $\Delta BVOL_{t-2}$ and $\Delta BVOL_{t-3}$ represent the lags of the changes of *BITVOL*. The positive return of Bitcoin is denoted by R_t^+, while the negative return of this cryptocurrency is denoted by R_t^-. Note that R_{t-1}^+, R_{t-2}^+ and R_{t-3}^+ are the lags of the positive returns. R_{t-1}^-, R_{t-2}^- and R_{t-3}^- are the lags of the negative returns. The significance levels at 1 %, 5 % and 10 % are denoted by ***, ** and *, respectively. The t-statistics are given in parentheses.

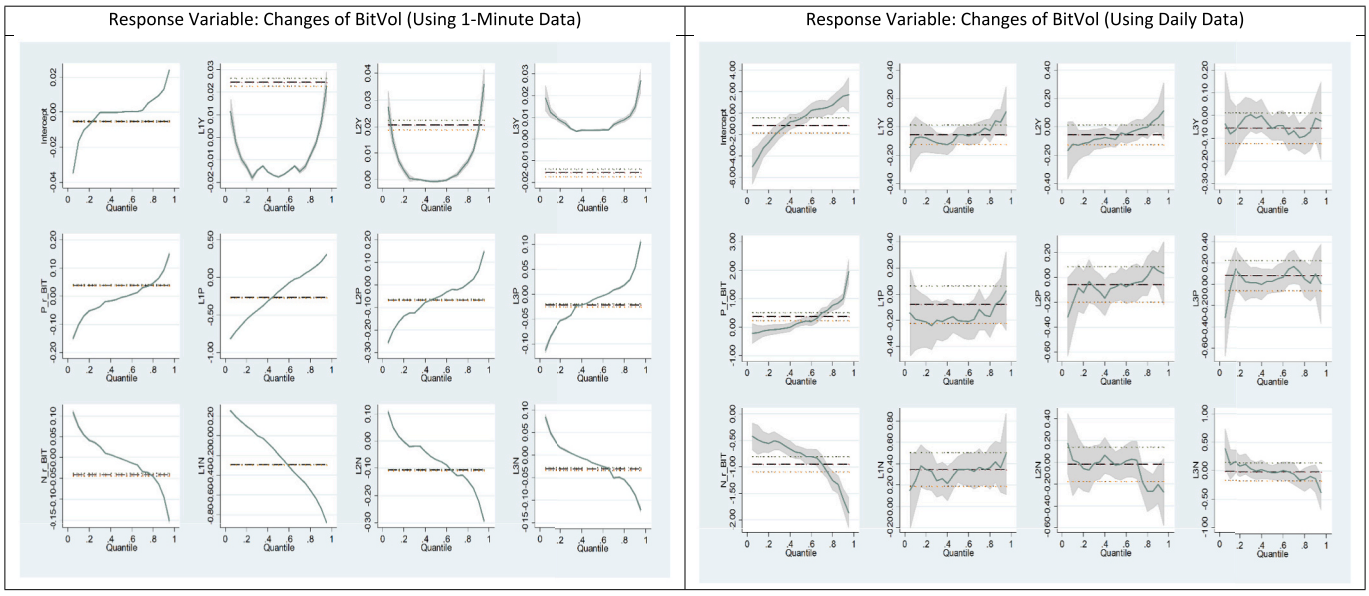

Fig. 1. QRM Plots of Bitcoin (Using 1-Minute and Daily Data).
Notes: P_r_BIT is the positive contemporaneous returns of Bitcoin, **L1p to L3P** are the lags of the positive returns, **N_r_BIT** is the negative contemporaneous returns of Bitcoin, and **L1N to L3N** are the lags of the negative returns.

method, applied to a time-series x_t with respect to the wavelet function Ψ, the continuous wavelet transform was formulated as a function of two variables:

$$W_x(a,b) = \int_{-\infty}^{\infty} x(t)\frac{1}{\sqrt{b}}\Psi\left(\frac{t-a}{b}\right)dt \tag{6}$$

In this context, the scale parameter, which governs the width of the wavelet, is represented by b, while the normalization factor is expressed as $\frac{1}{\sqrt{b}}$. Meanwhile, the time position parameter (a) dictates the wavelet's location. To estimate the continuous wavelet transform, the mother wavelet was applied to the chosen time series, denoted as $x(t) \in l^2(\mathrm{R})$, resulting in the estimation of $w_{x(a,b)}$.

Following Torrence and Webster (1999), the wavelet coherence of the two-time series $x(t)$ and $y(t)$ was expressed as follows:

$$\mathrm{R}_n^2(b) = \frac{\mathrm{I}B\left(b^{-1}W_n^{xy}(b)\right)\mathrm{I}^2}{B\left(b^{-1}\mathrm{I}W_n^{x}(b)\right)\mathrm{I}^2.B\left(b^{-1}\mathrm{I}W_n^{y}(b)\right)\mathrm{I}^2} \tag{7}$$

The scale parameter, responsible for regulating the width of the wavelet, is denoted as b. Additionally, the smoothing parameter is represented by B. The continuous wavelet transform of the time series x is denoted as $W_n^x(b)$, while that of the time series y is denoted as $W_n^y(b)$. Similarly, the cross wavelet transform of the time series x and y is indicated as $W_n^{xy}(b)$.

Drawing from the research conducted by Bloomfield et al. (2004), the phase discrepancy between the two time series, denoted as $x(t)$ and $y(t)$, was further characterized to explore the evolving interdependence and causality as outlined below:

$$\varnothing_{xy} = tan^{-1}\left(\frac{\Im\left\{\mathrm{B}\left(\mathrm{b}^{-1}\mathrm{W}_{xy}(\mathrm{a},\mathrm{b})\right)\right\}}{\Re\left\{\mathrm{B}\left(\mathrm{b}^{-1}\mathrm{W}_{xy}(\mathrm{a},\mathrm{b})\right)\right\}}\right), \quad \text{with } \psi_{xy} \in [-\pi,\pi] \tag{8}$$

When the arrow is positioned to the right, it signifies a positive relationship (in-phase) between the two time series, x(t) and y(t), whereas a leftward orientation indicates a negative relationship (anti-phase). Furthermore, arrows located at the top-left and bottom-right suggest that the time series y(t) precedes x(t). Conversely, arrows situated at the bottom-left and top-right indicate that x(t) leads y(t).

4. Empirical results

We discuss the empirical findings in this section. First, we highlight the results from the analysis of high-frequency (1-min) data, presented with suitable figures and tables. Subsequently, we discuss the relationship between changes in return volatility and variations in data frequency. Finally, we compare the results from low-frequency data (i.e., daily) with those from high-frequency data (i.e., 1 m, 5 m, 10 m, 15 m, and 60 m).

4.1. The intraday asymmetric relation between Bitcoin's (Ethereum's) returns and BitVol (EthVol) changes

For the relationship between BitVol changes and Bitcoin returns, we report the estimated results of QRM (Model-5) for 1-min and daily return intervals in Tables 2 and 3, respectively. Moreover, we show the corresponding QRM plots for the 1-min (daily) return interval in the left (right) panel of Fig. 1, with each of them having 12 covariates including an intercept. For each of the 12 covariates, we obtain 11 quantile regression coefficients (at q = 0.05…to 0.95).

Similarly, for the relation between EthVol changes and Ethereum returns, we display the estimated results of QRM for the 1-min (daily) return interval in Table 4 (Table 5), and the corresponding QRM plots for 1-min (left panel) and daily (right panel) return intervals are in Fig. 2. The 12th row of the above-mentioned tables reports the estimated results of OLS (Model-4).

In Fig. 3 (curved lines), we present successively for 1, 5, 10, 15, 60-min and daily data frequencies the contemporaneous conditional responses of BitVol and EthVol to the positive and negative return of Bitcoin and Ethereum, along with their 11 quantile-regression estimates,. The left (right) panels of Fig. 3 plot the return-volatility relationship of Bitcoin (Ethereum). The x-axis shows the 11 quantile parameters (q = 0.05…to 0.95), and the y-axis depicts the estimated effect in percentage. The estimated coefficients for each covariate can be interpreted as the conditional impact of percentage point changes of the covariate on the volatility changes, holding other covariates constant. The upward (downward) sloping dashed line with a circle-marked (diamond-marked) represents the coefficients of the cotemporaneous positive returns (negative returns). The absolute differences in the impact of positive and negative returns are presented with the dashed

Table 4
Testing the Changes of Ethereum Volatility Across the Quantiles at 1-Minute Data Frequency.

Quantile	$\Delta EVOL_{t-1}$	$\Delta EVOL_{t-2}$	$\Delta EVOL_{t-3}$	R_t^+	R_{t-1}^+	R_{t-2}^+	R_{t-3}^+	R_t^-	R_{t-1}^-	R_{t-2}^-	R_{t-3}^-	Intercept	R^2
0.05	0.00860***	0.0214***	0.0154***	−0.143***	−0.717***	−0.223***	−0.0936***	0.105***	0.234***	0.0814***	0.0682***	−0.0385***	0.0677
	(4.86)	(12.15)	(9.13)	(−62.45)	(−312.38)	(−96.18)	(−40.84)	(45.06)	(99.46)	(33.81)	(28.26)	(−134.50)	
0.1	−0.00251*	0.00984***	0.00843***	−0.0963***	−0.618***	−0.173***	−0.0721***	0.0775***	0.155***	0.0353***	0.0411***	−0.0220***	0.0678
	(−2.32)	(9.12)	(8.17)	(−68.45)	(−439.51)	(−122.06)	(−51.35)	(54.45)	(107.08)	(23.89)	(27.79)	(−125.30)	
0.15	−0.00781***	0.00472***	0.00652***	−0.0735***	−0.545***	−0.145***	−0.0579***	0.0609***	0.0956***	0.0104***	0.0277***	−0.0148***	0.0772
	(−9.48)	(5.76)	(8.31)	(−68.71)	(−509.49)	(−134.28)	(−54.24)	(56.29)	(87.05)	(9.29)	(24.60)	(−111.18)	
0.2	−0.0131***	0.00232***	0.00551***	−0.0554***	−0.483***	−0.125***	−0.0455***	0.0465***	0.0414***	−0.00605***	0.0157***	−0.0112***	0.0872
	(−18.94)	(3.38)	(8.37)	(−61.76)	(−538.91)	(−138.15)	(−50.76)	(51.20)	(44.93)	(−6.43)	(16.71)	(−100.49)	
0.25	−0.0168***	0.000218	0.00479***	−0.0420***	−0.431***	−0.109***	−0.0353***	0.0342***	−0.00190*	−0.0211***	0.00840***	−0.00873***	0.0609
	(−27.82)	(0.36)	(8.33)	(−53.45)	(−549.14)	(−137.54)	(−45.10)	(43.11)	(−2.35)	(−25.66)	(10.19)	(−89.33)	
Median	−0.0197***	−0.000372	0.00288***	−0.00458***	−0.196***	−0.0589***	−0.00715***	−0.000112	−0.203***	−0.0657***	−0.0117***	0.0000610	0.0011
	(−38.74)	(−0.73)	(5.93)	(−6.92)	(−297.16)	(−88.07)	(−10.83)	(−0.17)	(−298.47)	(−94.73)	(−16.85)	(0.74)	
0.75	−0.0139***	0.00281***	0.00707***	0.0309***	0.00492***	−0.0141***	0.0114***	−0.0303***	−0.432***	−0.115***	−0.0368***	0.00903***	0.0656
	(−23.16)	(4.70)	(12.35)	(39.62)	(6.31)	(−17.90)	(14.64)	(−38.35)	(−540.05)	(−140.63)	(−44.92)	(92.93)	
0.8	−0.00994***	0.00506***	0.00852***	0.0452***	0.0507***	−0.0000227	0.0204***	−0.0447***	−0.487***	−0.133***	−0.0466***	0.0110***	0.0953
	(−14.68)	(7.51)	(13.20)	(51.36)	(57.67)	(−0.03)	(23.21)	(−50.26)	(−539.75)	(−143.85)	(−50.45)	(99.91)	
0.85	−0.00569***	0.00783***	0.00967***	0.0632***	0.109***	0.0173***	0.0310***	−0.0621***	−0.553***	−0.154***	−0.0596***	0.0137***	0.1306
	(−7.20)	(9.95)	(12.85)	(61.57)	(106.07)	(16.64)	(30.24)	(−59.85)	(−525.05)	(−143.02)	(−55.29)	(107.46)	
0.9	−0.000128	0.0130***	0.0125***	0.0890***	0.176***	0.0438***	0.0457***	−0.0879***	−0.638***	−0.183***	−0.0730***	0.0189***	0.1712
	(−0.12)	(12.44)	(12.42)	(65.03)	(128.78)	(31.73)	(33.46)	(−63.54)	(−454.74)	(−127.39)	(−50.79)	(111.18)	
0.95	0.00892***	0.0222***	0.0156***	0.130***	0.269***	0.0914***	0.0793***	−0.137***	−0.765***	−0.241***	−0.102***	0.0312***	0.2156
	(5.20)	(12.98)	(9.55)	(58.21)	(120.71)	(40.62)	(35.70)	(−60.91)	(−334.66)	(−103.30)	(−43.51)	(112.63)	
OLS	0.0179	0.0198	−0.0178	0.0443	−0.225***	−0.0580***	−0.0461	−0.0386**	−0.258***	−0.0855***	−0.00888	−0.00439**	0.13738
	(1.16)	(1.49)	(−0.79)	(1.05)	(−10.04)	(−4.48)	(−1.49)	(−2.63)	(−15.30)	(−6.32)	(−0.53)	(−2.82)	

Notes: We provide the results from the lower to upper (i.e., 0.05 to 0.95) quantile regressions and the OLS regression of the changes of *ETHVOL* on the set of independent variables. The variables $\Delta EVOL_{t-1}$, $\Delta EVOL_{t-2}$ and $\Delta EVOL_{t-3}$ represent the lags of the changes of *ETHVOL*. The positive return of Ethereum is denoted by R_t^+, while the negative return of this crypto is denoted by R_t^-. Note that R_{t-1}^+, R_{t-2}^+ and R_{t-3}^+ are the lags of the positive return, while R_{t-1}^-, R_{t-2}^- and R_{t-3}^- are the lags of the negative return. The significance levels at 1 %, 5 % and 10 % are denoted by ***, ** and *, respectively. *The t*-statistics are given in parentheses.

Table 5
Testing the Changes of Ethereum Volatility Across the Quantiles at Daily Data Frequency.

Quantile	$\Delta EVOL_{t-1}$	$\Delta EVOL_{t-2}$	$\Delta EVOL_{t-3}$	R_t^+	R_{t-1}^+	R_{t-2}^+	R_{t-3}^+	R_t^-	R_{t-1}^-	R_{t-2}^-	R_{t-3}^-	Intercept	R^2
0.05	−0.128	−0.167*	−0.0926	−0.299	−0.120	0.127	−0.0718	−0.226	0.204	−0.0636	0.0234	−6.431***	0.1309
	(−1.51)	(−1.97)	(−1.12)	(−1.89)	(−0.76)	(0.81)	(−0.46)	(−1.46)	(1.17)	(−0.36)	(0.13)	(−6.50)	
0.1	−0.129*	−0.158**	−0.0518	−0.108	−0.104	−0.0518	0.0979	−0.175	0.303*	0.0389	0.0949	−4.396***	0.0844
	(−2.12)	(−2.61)	(−0.88)	(−0.96)	(−0.92)	(−0.46)	(0.88)	(−1.57)	(2.43)	(0.31)	(0.75)	(−6.20)	
0.15	−0.0880	−0.147**	−0.0535	−0.200*	−0.0777	−0.0363	0.0860	−0.220**	0.324***	−0.00577	0.0582	−3.297***	0.0684
	(−1.91)	(−3.20)	(−1.19)	(−2.33)	(−0.90)	(−0.43)	(1.02)	(−2.60)	(3.43)	(−0.06)	(0.61)	(−6.13)	
0.2	−0.123**	−0.120**	−0.0549	−0.189**	−0.0625	−0.0240	0.0483	−0.301***	0.291***	−0.00585	0.0825	−2.729***	0.0622
	(−3.29)	(−3.21)	(−1.50)	(−2.72)	(−0.89)	(−0.35)	(0.70)	(−4.40)	(3.80)	(−0.08)	(1.06)	(−6.25)	
0.25	−0.101*	−0.102*	−0.0552	−0.175*	−0.0532	−0.0357	0.0128	−0.350***	0.301***	0.00896	0.107	−2.181***	0.0542
	(−2.57)	(−2.57)	(−1.43)	(−2.37)	(−0.72)	(−0.49)	(0.18)	(−4.82)	(3.70)	(0.11)	(1.30)	(−4.72)	
Median	−0.0456	−0.0296	0.0209	0.165*	−0.0675	−0.0731	−0.0795	−0.727***	0.187*	0.105	0.111	−0.444	0.0644
	(−1.24)	(−0.80)	(0.58)	(2.39)	(−0.97)	(−1.07)	(−1.17)	(−10.73)	(2.46)	(1.37)	(1.44)	(−1.03)	
0.75	−0.000379	−0.0352	−0.0129	0.494***	−0.0495	−0.0129	−0.0426	−1.093***	0.280***	0.127	0.0576	0.832	0.1119
	(−0.01)	(−0.88)	(−0.33)	(6.60)	(−0.66)	(−0.17)	(−0.58)	(−14.86)	(3.40)	(1.53)	(0.69)	(1.77)	
0.8	0.0410	−0.0481	−0.0255	0.592***	0.0168	0.000268	−0.0332	−1.153***	0.308**	0.0892	0.0619	1.032	0.1205
	(0.80)	(−0.94)	(−0.51)	(6.21)	(0.18)	(0.00)	(−0.35)	(−12.31)	(2.93)	(0.84)	(0.58)	(1.73)	
0.85	0.0708	−0.0145	−0.0466	0.674***	0.00989	0.0467	0.0301	−1.306***	0.394***	0.0150	0.0143	1.239	0.1448
	(1.26)	(−0.26)	(−0.85)	(6.40)	(0.09)	(0.45)	(0.29)	(−12.63)	(3.40)	(0.13)	(0.12)	(1.88)	
0.9	0.0416	−0.0309	−0.0592	0.837***	0.0983	−0.0607	−0.0381	−1.504***	0.320*	0.100	0.0613	2.258**	0.207
	(0.57)	(−0.42)	(−0.83)	(6.12)	(0.71)	(−0.45)	(−0.28)	(−11.19)	(2.13)	(0.66)	(0.40)	(2.63)	
0.95	−0.0111	0.00895	−0.0645	1.324***	0.245	0.229	−0.0270	−1.800***	0.203	0.100	0.0716	2.641	0.3333
	(−0.08)	(0.07)	(−0.50)	(5.39)	(0.99)	(0.94)	(−0.11)	(−7.46)	(0.75)	(0.37)	(0.26)	(1.72)	
OLS	−0.0424	−0.0484	−0.0152	0.359**	0.0542	0.0192	−0.0847	−0.983***	0.292***	0.0408	0.166*	−1.326*	0.222
	(−0.96)	(−1.24)	(−0.42)	(3.14)	(0.44)	(0.32)	(−1.32)	(−5.03)	(3.74)	(0.53)	(2.04)	(−2.46)	

Notes: We provide the results from the lower to upper (i.e., 0.05 to 0.95) quantile regressions and the OLS regression of the changes of *ETHVOL* on the set of independent variables. The variables $\Delta EVOL_{t-1}$, $\Delta EVOL_{t-2}$ and $\Delta EVOL_{t-3}$ represent the lags of the changes of *ETHVOL*. The positive return of Ethereum is denoted by R_t^+, while the negative return of this crypto is denoted by R_t^-. Note that R_{t-1}^+, R_{t-2}^+ and R_{t-3}^+ are the lags of the positive return, while R_{t-1}^-, R_{t-2}^- and R_{t-3}^- are the lags of the negative return. The significance levels at 1 %, 5 % and 10 % are denoted by ***, ** and *, respectively. *The t*-statistics are given in parentheses.

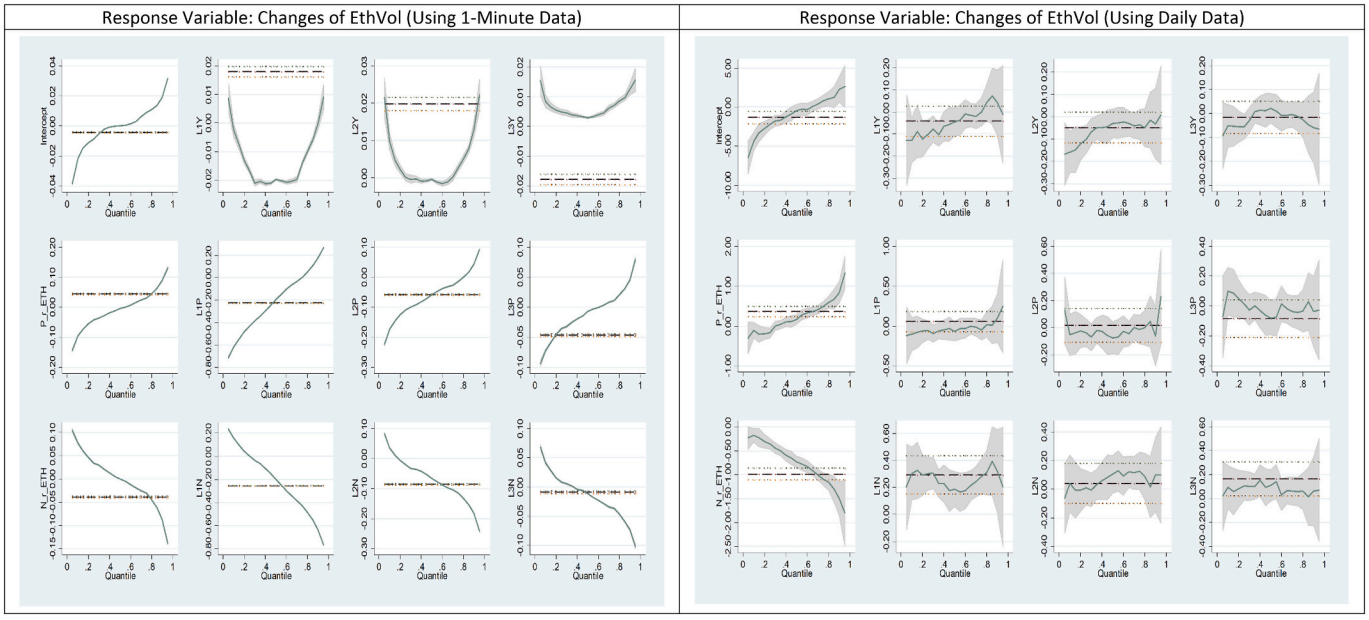

Fig. 2. QRM Plots of Ethereum (Using 1-Minute and Daily Data).
Notes: P_r_ETH is the positive contemporaneous returns of Ethereum, **L1p to L3P** are the lags of the positive returns, **N_r_ETH** is the negative contemporaneous returns of Ethereum, and **L1N to L3N** are the lags of the negative returns.

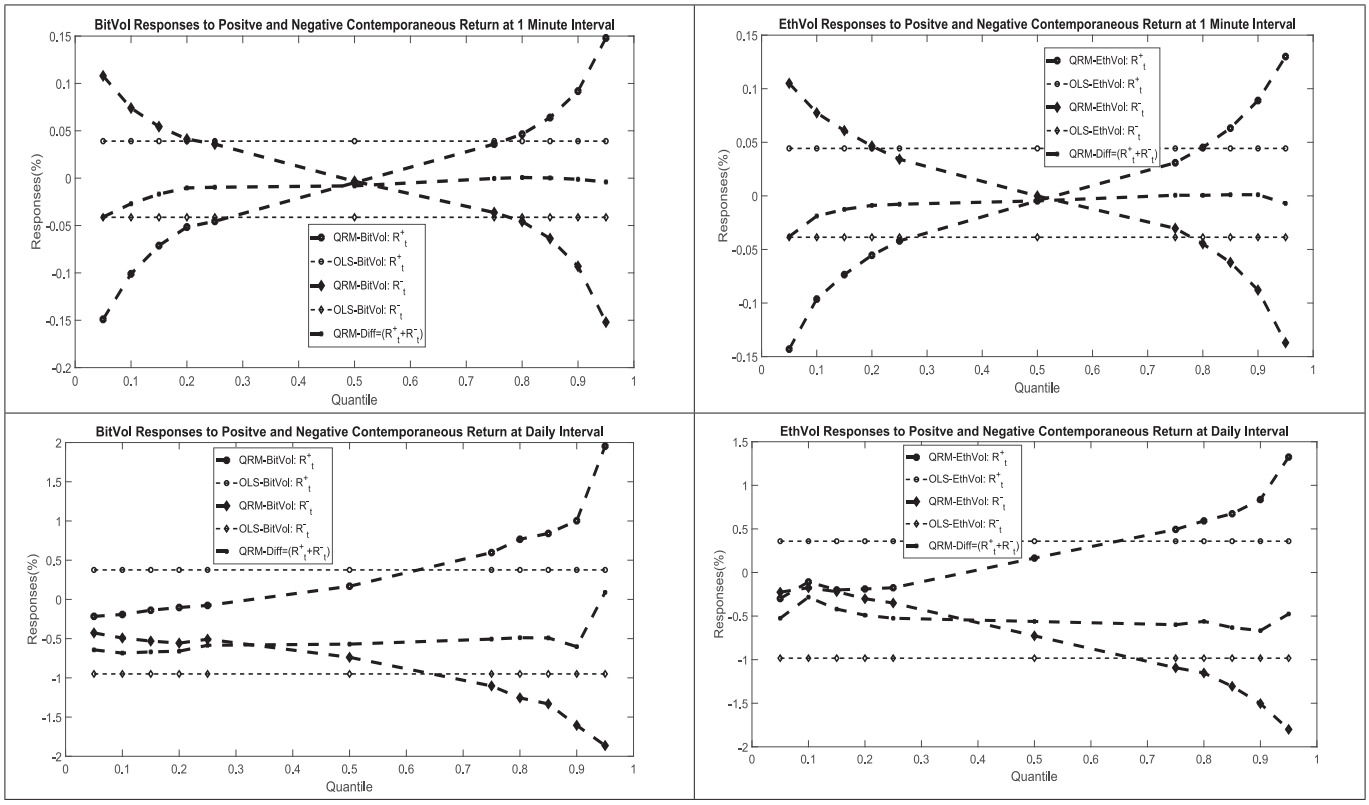

Fig. 3. Asymmetric Responses of Δ*EthVol* and Δ*BitVol* to Positive and Negative Return of Bitcoin and Ethereum.

line with a small square-shaped. The straight dotted lines represent the estimated coefficient from the standard robust OLS (Model-4).

We report the results of Bitcoin's (Ethereum's) return-volatility relationship for 1-min data frequency in Table 2 (Table 4), Fig. 1 (Fig. 2) and the upper-left (upper-right) panel of Fig. 3. Noticeably, the coefficients of the contemporaneous effect of positive returns estimated using QRM were negative at the lowest to medium quantiles (q = 0.05 to 0.5), and the magnitude of the negative coefficients monotonically decreases as we move to the upper quantiles of the volatility distribution. Consequently, the contemporaneous effect showed positive signs at medium to the uppermost quantiles (q = 0.5 to 0.95), and the positive effect monotonically increases as we move from medium to the

Table 6
Quantile Regression Combined Results: Response Variable is Changes of BitVol (1, 5, 10, 15, 60 Minutes and Daily)

$$\Delta BVOL_{it} = \alpha^{(q)} + \sum_{L=1}^{3} \beta_{i\,L}^{(q)} L\Delta BVOL_{it-L} + \sum_{L=0}^{3} \gamma_{i\,L}^{(q)} R_{it-L}^{+} + \sum_{L=0}^{3} \delta_{i\,L}^{(q)} R_{it-L}^{-} + u_t$$

	Quantile	$\Delta BVOL_{t-1}$	$\Delta BVOL_{t-2}$	$\Delta BVOL_{t-3}$	R_t^+	R_{t-1}^+	R_{t-2}^+	R_{t-3}^+	R_t^-	R_{t-1}^-	R_{t-2}^-	R_{t-3}^-	intercept	R^2
1 m	0.05	0.0113***	0.0274***	0.0188***	−0.149***	−0.813***	−0.255***	−0.112***	0.108***	0.253***	0.106***	0.0838***	−0.0347***	0.1014
5 m	0.05	0.0298***	0.0436***	0.0211***	−0.709***	−0.350***	−0.120***	−0.111***	0.142***	0.135***	0.184***	0.154***	−0.112***	0.1172
10 m	0.05	0.0606***	0.0358***	0.0224***	−0.751***	−0.225***	−0.101***	−0.106***	0.117***	0.219***	0.153***	0.154***	−0.179***	0.1031
15 m	0.05	0.0769***	0.0444***	0.0289***	−0.711***	−0.182***	−0.149***	−0.126***	0.102***	0.204***	0.207***	0.145***	−0.223***	0.0926
60 m	0.05	0.127***	−0.00402	−0.0364*	−0.543***	−0.194***	−0.196***	−0.165***	0.0567	0.326***	0.294***	0.146***	−0.571***	0.0672
Daily	0.05	−0.146	−0.167	−0.0369	−0.216	−0.146	−0.317	−0.311	−0.427*	0.149	0.172	0.384	−4.982***	0.1554
1 m	0.10	−0.00265**	0.0143***	0.0122***	−0.101***	−0.716***	−0.201***	−0.0853***	0.0740***	0.191***	0.0491***	0.0489***	−0.0163***	0.0875
5 m	0.10	0.0167***	0.0363***	0.0253***	−0.604***	−0.298***	−0.0784***	−0.0720***	0.0525***	0.0644***	0.117***	0.0972***	−0.0680***	0.0946
10 m	0.10	0.0398***	0.0325***	0.0255***	−0.654***	−0.181***	−0.0756***	−0.0738***	0.0123	0.136***	0.104***	0.122***	−0.112***	0.0828
15 m	0.10	0.0569***	0.0455***	0.0252***	−0.623***	−0.131***	−0.0650***	−0.0796***	−0.00302	0.110***	0.152***	0.101***	−0.151***	0.074
60 m	0.10	0.107***	−0.00241	−0.0199	−0.491***	−0.112***	−0.145***	−0.0990***	−0.0730***	0.229***	0.170***	0.105***	−0.393***	0.0486
Daily	0.10	−0.0795	−0.123	−0.0810	−0.192	−0.194	−0.201	−0.0363	−0.492***	0.240	0.0196	0.108	−4.172***	0.1044
1 m	0.15	−0.00981***	0.00697***	0.0101***	−0.0712***	−0.630***	−0.163***	−0.0668***	0.0544***	0.141***	0.0165***	0.0285***	−0.0103***	0.0756
5 m	0.15	0.00237	0.0291***	0.0246***	−0.538***	−0.253***	−0.0617***	−0.0472***	0.000613	0.0247***	0.0885***	0.0803***	−0.0469***	0.0784
10 m	0.15	0.0325***	0.0314***	0.0250***	−0.584***	−0.153***	−0.0460***	−0.0472***	−0.0435***	0.0855***	0.0918***	0.101***	−0.0799***	0.0691
15 m	0.15	0.0521***	0.0361***	0.0196***	−0.547***	−0.0912***	−0.0411***	−0.0655***	−0.0685***	0.0707***	0.115***	0.0827***	−0.114***	0.0632
60 m	0.15	0.0943***	−0.00764	−0.00584	−0.449***	−0.0672***	−0.0886***	−0.0765***	−0.151***	0.178***	0.125***	0.0751***	−0.308***	0.0402
Daily	0.15	−0.0707	−0.129*	−0.0629	−0.138	−0.203	−0.0850	0.144	−0.531***	0.377**	−0.00112	0.163	−3.285***	0.0737
1 m	0.20	−0.0131***	0.00354***	0.00844***	−0.0516***	−0.553***	−0.138***	−0.0527***	0.0413***	0.0936***	−0.00306**	0.0171***	−0.00717***	0.0654
5 m	0.20	−0.00178	0.0250***	0.0221***	−0.488***	−0.218***	−0.0464***	−0.0372***	−0.0356***	−0.00241	0.0659***	0.0648***	−0.0332***	0.0635
10 m	0.20	0.0269***	0.0336***	0.0249***	−0.532***	−0.126***	−0.0295***	−0.0281***	−0.0988***	0.0542***	0.0699***	0.0858***	−0.0610***	0.0569
15 m	0.20	0.0474***	0.0361***	0.0207***	−0.498***	−0.0737***	−0.0145**	−0.0580***	−0.127***	0.0512***	0.101***	0.0743***	−0.0875***	0.0536
60 m	0.20	0.0907***	−0.00173	−0.00818	−0.399***	−0.0528***	−0.0823***	−0.0697***	−0.208***	0.149***	0.109***	0.0625***	−0.239***	0.0341
Daily	0.20	−0.0792	−0.116**	−0.0382	−0.103	−0.214*	−0.122	0.0942	−0.557***	0.344***	−0.0577	0.0895	−2.716***	0.0726
1 m	0.25	−0.0181***	0.000545	0.00718***	−0.0455***	−0.490***	−0.124***	−0.0491***	0.0359***	0.0534***	−0.0205***	0.0108***	−0.00366***	0.0554
5 m	0.25	−0.00706***	0.0213***	0.0206***	−0.439***	−0.186***	−0.0356***	−0.0290***	−0.0654***	−0.0274***	0.0543***	0.0529***	−0.0238***	0.0502
10 m	0.25	0.0205***	0.0300***	0.0225***	−0.481***	−0.0965***	−0.0173***	−0.0185***	−0.136***	0.0255***	0.0580***	0.0724***	−0.0476***	0.0462
15 m	0.25	0.0408***	0.0351***	0.0210***	−0.459***	−0.0641***	0.000402	−0.0447***	−0.165***	0.0298***	0.0844***	0.0661***	−0.0670***	0.045
60 m	0.25	0.0848***	0.00299	−0.00735	−0.378***	−0.0318**	−0.0758***	−0.0483***	−0.252***	0.125***	0.0988***	0.0443***	−0.187***	0.0303
Daily	0.25	−0.0961*	−0.110**	−0.00660	−0.0768	−0.242**	−0.0317	0.0281	−0.508***	0.327***	−0.0704	0.124	−2.104***	0.0812
1 m	0.50	−0.0176***	−0.000746	0.00398***	−0.00477***	−0.191***	−0.0582***	−0.0117***	−0.00333***	−0.192***	−0.0677***	−0.0164***	0.0000786	0.0134
5 m	0.50	−0.0108***	0.0162***	0.0158***	−0.220***	−0.0792***	0.00558**	0.00378*	−0.220***	−0.113***	0.00964***	0.0165***	−0.000325	0.0121
10 m	0.50	0.0167***	0.0286***	0.0196***	−0.271***	−0.0160***	0.0132***	0.0101***	−0.315***	−0.0547***	0.0203***	0.0310***	−0.00486***	0.0198
15 m	0.50	0.0377***	0.0385***	0.0239***	−0.260***	−0.00426	0.0349***	−0.00855*	−0.357***	−0.0269***	0.0340***	0.0372***	−0.00868***	0.025
60 m	0.50	0.0834***	0.00945*	−0.000831	−0.187***	0.0517***	−0.0433***	−0.00980	−0.464***	0.0255**	0.0544***	0.0302***	−0.0464***	0.0282
Daily	0.50	−0.0560	−0.0879**	−0.0578	0.168*	−0.206**	−0.0767	0.0322	−0.738***	0.346***	−0.0284	−0.0244	−0.515	0.0893
1 m	0.75	−0.0130***	0.00455***	0.00799***	0.0360***	0.0523***	−0.0119***	0.0123***	−0.0363***	−0.483***	−0.126***	−0.0486***	0.00506***	0.0625
5 m	0.75	0.00348**	0.0290***	0.0219***	−0.0368***	0.0153***	0.0455***	0.0440***	−0.457***	−0.230***	−0.0285***	−0.0205***	0.0166***	0.0605
10 m	0.75	0.0393***	0.0384***	0.0290***	−0.0413***	0.0691***	0.0489***	0.0413***	−0.554***	−0.150***	−0.0149***	−0.00181	0.0268***	0.0671
15 m	0.75	0.0529***	0.0433***	0.0290***	−0.0438***	0.0713***	0.0577***	0.0228***	−0.579***	−0.107***	0.000397	0.000878	0.0393***	0.0665
60 m	0.75	0.116***	0.0259***	0.0116*	0.0696***	0.142***	−0.0103	0.00637	−0.737***	−0.0227	0.0343**	0.0229	0.0956***	0.0613
Daily	0.75	−0.00991	−0.00868	−0.0961*	0.597***	−0.164	−0.0331	0.121	−1.103***	0.342**	−0.178	−0.154	0.509	0.1464
1 m	0.80	−0.00801***	0.00683***	0.00887***	0.0464***	0.0952***	0.00570***	0.0182***	−0.0457***	−0.552***	−0.144***	−0.0542***	0.00733***	0.0756
5 m	0.80	0.0114***	0.0342***	0.0255***	0.00517	0.0487***	0.0576***	0.0563***	−0.516***	−0.269***	−0.0406***	−0.0268***	0.0225***	0.0806
10 m	0.80	0.0480***	0.0431***	0.0332***	0.00776	0.0967***	0.0599***	0.0579***	−0.609***	−0.179***	−0.0256***	−0.00892*	0.0368***	0.0854
15 m	0.80	0.0655***	0.0467***	0.0317***	0.0141**	0.0935***	0.0666***	0.0394***	−0.640***	−0.133***	−0.00706	−0.0143**	0.0523***	0.0833
60 m	0.80	0.126***	0.0283***	0.0161*	0.133***	0.170***	−0.00562	0.00819	−0.816***	−0.0506**	0.0190	0.0186	0.134***	0.0772
Daily	0.80	−0.0264	−0.00200	−0.0913*	0.767***	−0.173	0.0112	0.0515	−1.255***	0.361***	−0.266**	−0.150	0.716	0.1759
1 m	0.85	−0.00255***	0.0109***	0.0106***	0.0640***	0.148***	0.0264***	0.0297***	−0.0638***	−0.636***	−0.172***	−0.0688***	0.00949***	0.0976
5 m	0.85	0.0226***	0.0426***	0.0312***	0.0575***	0.0889***	0.0723***	0.0794***	−0.578***	−0.320***	−0.0541***	−0.0367***	0.0312***	0.1043
10 m	0.85	0.0632***	0.0480***	0.0396***	0.0716***	0.128***	0.0762***	0.0715***	−0.690***	−0.215***	−0.0467***	−0.0177***	0.0511***	0.1076
15 m	0.85	0.0812***	0.0503***	0.0386***	0.0849***	0.138***	0.0899***	0.0511***	−0.711***	−0.169***	−0.0192**	−0.0220**	0.0690***	0.1027
60 m	0.85	0.140***	0.0206*	0.0189*	0.235***	0.249***	−0.00808	0.00832	−0.937***	−0.100***	0.00923	0.0283	0.182***	0.1017

(*continued on next page*)

Table 6 (*continued*)

$$\Delta BVOL_{tt} = \alpha^{(q)} + \sum_{L=1}^{3} \beta_L^{(q)} L\Delta BVOL_{tt-L} + \sum_{L=0}^{3} \gamma_L^{(q)} R_{tt-L}^{+} + \sum_{L=0}^{3} \delta_L^{(q)} R_{tt-L}^{-} + u_t$$

	Quantile	$\Delta BVOL_{t-1}$	$\Delta BVOL_{t-2}$	$\Delta BVOL_{t-3}$	R_t^+	R_{t-1}^+	R_{t-2}^+	R_{t-3}^+	R_t^-	R_{t-1}^-	R_{t-2}^-	R_{t-3}^-	intercept	R^2
Daily	0.85	0.0408	0.0379	−0.0705	0.841***	−0.0810	0.0881	0.0145	−1.332***	0.417***	−0.265*	−0.0947	1.201*	0.212
1 m	0.90	0.00598***	0.0186***	0.0146***	0.0919***	0.208***	0.0639***	0.0538***	−0.0931***	−0.734***	−0.219***	−0.0877***	0.0131***	0.1256
5 m	0.90	0.0410***	0.0500***	0.0398***	0.120***	0.150***	0.0937***	0.105***	−0.672***	−0.386***	−0.0780***	−0.0520***	0.0456***	0.1329
10 m	0.90	0.0852***	0.0587***	0.0458***	0.155***	0.181***	0.103***	0.110***	−0.779***	−0.265***	−0.0719***	−0.0378***	0.0733***	0.1367
15 m	0.90	0.0981***	0.0603***	0.0456***	0.177***	0.191***	0.115***	0.0767***	−0.811***	−0.217***	−0.0320***	−0.0414***	0.0978***	0.1281
60 m	0.90	0.142***	0.0131	0.0240*	0.363***	0.315***	−0.00522	0.0255	−1.070***	−0.151***	−0.00598	0.00504	0.255***	0.1393
Daily	0.90	0.0335	0.0654	−0.0114	1.003***	−0.0481	0.0524	0.0982	−1.605***	0.362	−0.206	−0.131	1.555	0.2722
1 m	0.95	0.0227***	0.0359***	0.0268***	0.148***	0.300***	0.146***	0.105***	−0.152***	−0.876***	−0.292***	−0.120***	0.0238***	0.1678
5 m	0.95	0.0736***	0.0711***	0.0464***	0.243***	0.269***	0.143***	0.149***	−0.813***	−0.509***	−0.109***	−0.0911***	0.0783***	0.1722
10 m	0.95	0.124***	0.0752***	0.0548***	0.336***	0.281***	0.151***	0.145***	−0.920***	−0.363***	−0.118***	−0.0956***	0.120***	0.1807
15 m	0.95	0.138***	0.0715***	0.0585***	0.392***	0.329***	0.172***	0.110***	−0.960***	−0.334***	−0.0678***	−0.0670***	0.151***	0.1747
60 m	0.95	0.180***	0.0348	0.0132	0.625***	0.485***	0.0546	0.0858*	−1.278***	−0.329***	−0.0232	−0.0167	0.371***	0.2058
Daily	0.95	0.107	0.111	−0.0240	1.953***	0.0223	0.0328	0.00841	−1.863***	0.490**	−0.274	−0.373*	1.683*	0.3486
1 m	OLS	0.0244	0.0206	−0.0155	0.0391	−0.267***	−0.0666***	−0.0220	−0.0413**	−0.293***	−0.107***	−0.0308	−0.00512***	0.0567
5 m	OLS	−0.0373	0.00573	0.00776	−0.243***	−0.0239	−0.0208	−0.0403*	−0.324***	−0.333***	0.0308	0.0737***	−0.0168**	0.0694
10 m	OLS	0.0331	0.0410*	0.0243*	−0.221***	0.0364	−0.0335	−0.0111	−0.436***	−0.174*	0.0625	0.0585*	−0.0271**	0.0686
15 m	OLS	−0.0193	0.0443**	0.0355**	−0.204***	−0.0213	0.0313*	−0.0259	−0.565***	−0.0456	0.0531*	0.0623**	−0.0354**	0.074
60 m	OLS	0.110***	0.0138	−0.0416	−0.0776	0.0888*	−0.0881***	−0.0449*	−0.673***	0.0318	0.0972***	0.0433	−0.0942***	0.0911
Daily	OLS	−0.0557	−0.0556	−0.0552	0.376**	−0.0820	−0.0570	0.0841	−0.950***	0.345***	−0.0181	−0.0121	−1.145**	0.2037

Notes: This table provides findings from the lower to upper quantiles regression (0.05 to 0.95) and OLS regression for Bitcoin. The results for all six time-intervals are grouped according to each q-value. R_t^+ and R_t^- represent the impact of contemporaneous positive and negative returns of Bitcoin. R_{t-l}^+ and R_{t-l}^- represent the impact of lags of positive and negative returns of Bitcoin. $\Delta BVOL_{t-1}$, $\Delta BVOL_{t-2}$ and $\Delta BVOL_{t-3}$ are the lags of the dependent variable (changes of BitVol). The significance level at 1 %, 5 % and 10 % are denoted by ***, ** and *, respectively.

uppermost quantile of the volatility distributions. On the other hand, the corresponding OLS estimate showed a positive effect, but the magnitude of the effect is less than the corresponding QRM estimates. Moreover, over the range of quantiles, there is a considerable variation in the positive return-volatility relationship. The estimated coefficients of contemporaneous positive returns of Bitcoin (Ethereum) vary from −0.148 (−0.143) at the lowest quantile to +0.149 (+0.130) at the uppermost quantile and are statistically significant. This implies that, during the low to medium volatility regimes, cryptocurrencies' volatility (BitVol and EthVol) is negatively associated with their respective cryptocurrencies' positive returns (Bitcoin and Ethereum) at the 1-min holding period. In contrast, during the medium to high volatility regimes, cryptocurrencies' volatility (BitVol and EthVol) is positively associated with their respective cryptocurrencies' positive returns (Bitcoin and Ethereum) at the 1-min holding period. Moreover, the impact of positive return on the changes of volatility was more pronounced at extreme tails of the volatility distributions. The autocorrelation—denoted by the coefficients of the lags of the changes of BitVol (in Table 2) and EthVol (in Table 4)—are robust and highly significant over the range of different quantiles. Also, the cross-autocorrelation with positive returns—denoted by the coefficients of the lags of Bitcoin (in Table 2) and Ethereum's positive returns (in Table 4)—are highly significant across the quantiles for all lags. Even though the size of the coefficients of contemporaneous positive returns was bigger than the size of the coefficients of the positive lag returns, the signs of the coefficients were the same. Hence, the cross-autocorrelation was negatively significant at the lowermost (q = 0.05) to medium (q = 0.5) quantiles of the distribution. However, the relationship changes to positive after the medium quantile. The magnitude of the positive (negative) effect monotonically increases (decreases) as we move from medium to the uppermost quantile of the volatility distributions. Again, the corresponding OLS estimates either overestimate or underestimate the cross-autocorrelation observed over the range of different quantiles.

The figure of the contemporaneous effect of negative returns on changes of BitVol (EthVol) in the upper-right (upper-left) panel of Fig. 3 displays a mirror image of the results of positive returns. The coefficients of the contemporaneous effect of negative returns estimated using QRM were positive at the lowest to medium quantiles (q = 0.05 to 0.5), and the magnitude of the positive coefficients monotonically decreases as we move to the medium quantiles of the volatility distribution. Accordingly, the contemporaneous effect showed that the negative signs at medium to the uppermost quantiles (q = 0.5 to 0.95), and the size of the negative coefficients monotonically increases as we move from medium to the uppermost quantile of the volatility distributions. On the other hand, the estimated coefficients of the corresponding OLS showed negative signs, and the magnitude of the effect is less than the corresponding QRM estimates. Moreover, over the range of quantiles, there is a considerable variation in the negative return-volatility relationship. The estimated coefficients of contemporaneous positive returns of Bitcoin (Ethereum) vary from 0.108 (0.105) at the lowest quantile to −0.152 (−0.137) at the uppermost quantile and are statistically significant. Similar to the finding from positives returns, it also implies that, during the low to medium volatility regimes, cryptocurrencies' volatility (BitVol and EthVol) is negatively associated with their respective cryptocurrencies' negative returns (Bitcoin and Ethereum) at the 1-min holding period. In contrast, during the medium to high volatility regimes, cryptocurrencies' volatility (BitVol and EthVol) is positively associated with their respective cryptocurrencies' positive returns (Bitcoin and Ethereum) at the 1-min holding period. Moreover, the impact of negative return on the changes of volatility is more pronounced at extreme tails of the volatility distributions. Similar to the finding of positive returns, the autocorrelation structure of negative returns is also robust and highly significant over the range of different quantiles. The cross-autocorrelation with negative returns is highly significant across the quantiles for all lags, and the signs (size) of the coefficients are the same (smaller) as (than) the signs (size) of coefficients of contemporaneous returns.

Table 7
Quantile Regression Combined Results: Response Variable is Changes of EthVol (1, 5, 10, 15, 60 Minutes and Daily)

$$\Delta EVOL_{it} = \alpha^{(q)} + \sum_{L=1}^{3} \beta_{i\,L}^{(q)} L\Delta EVOL_{it-L} + \sum_{L=0}^{3} \gamma_{i\,L}^{(q)} R_{it-L}^{+} + \sum_{L=0}^{3} \delta_{i\,L}^{(q)} R_{it-L}^{-} + u_t$$

	Quantile	$\Delta EVOL_{t-1}$	$\Delta EVOL_{t-2}$	$\Delta EVOL_{t-3}$	R_t^+	R_{t-1}^+	R_{t-2}^+	R_{t-3}^+	R_t^-	R_{t-1}^-	R_{t-2}^-	R_{t-3}^-	intercept	R^2
1 m	0.05	0.00860***	0.0214***	0.0154***	−0.143***	−0.717***	−0.223***	−0.0936***	0.105***	0.234***	0.0814***	0.0682***	−0.0385***	0.1245
5 m	0.05	0.0184***	0.0296***	0.0296***	−0.684***	−0.319***	−0.102***	−0.0820***	0.187***	0.142***	0.150***	0.128***	−0.103***	0.1376
10 m	0.05	0.0489***	0.0423***	0.0222**	−0.721***	−0.204***	−0.106***	−0.0948***	0.205***	0.176***	0.148***	0.125***	−0.162***	0.1202
15 m	0.05	0.0902***	0.0280***	0.0000754	−0.639***	−0.160***	−0.111***	−0.107***	0.186***	0.207***	0.163***	0.137***	−0.219***	0.1131
60 m	0.05	0.0901***	0.0111	0.00879	−0.571***	−0.221***	−0.122***	−0.155***	0.107***	0.213***	0.109**	0.117***	−0.624***	0.0512
Daily	0.05	−0.128	−0.167*	−0.0926	−0.299	−0.120	0.127	−0.0718	−0.226	0.204	−0.0636	0.0234	−6.431***	0.1309
1 m	0.10	−0.00251*	0.00984***	0.00843***	−0.0963***	−0.618***	−0.173***	−0.0721***	0.0775***	0.155***	0.0353***	0.0411***	−0.0220***	0.1054
5 m	0.10	−0.00394	0.0209***	0.0210***	−0.593***	−0.263***	−0.0668***	−0.0532***	0.102***	0.0669***	0.0952***	0.0867***	−0.0625***	0.1145
10 m	0.10	0.0214***	0.0377***	0.0154***	−0.635***	−0.137***	−0.0598***	−0.0642***	0.0974***	0.0903***	0.104***	0.104***	−0.101***	0.101
15 m	0.10	0.0577***	0.0223***	0.00169	−0.590***	−0.134***	−0.0702***	−0.0612***	0.0688***	0.134***	0.111***	0.0875***	−0.139***	0.0925
60 m	0.10	0.0759***	0.0132	−0.00780	−0.492***	−0.129***	−0.0891***	−0.0991***	−0.00104	0.172***	0.0845***	0.0584**	−0.425***	0.0453
Daily	0.10	−0.129*	−0.158**	−0.0518	−0.108	−0.104	−0.0518	0.0979	−0.175	0.303*	0.0389	0.0949	−4.396***	0.0844
1 m	0.15	−0.00781***	0.00472***	0.00652***	−0.0735***	−0.545***	−0.145***	−0.0579***	0.0609***	0.0956***	0.0104***	0.0277***	−0.0148***	0.8456
5 m	0.15	−0.0140***	0.0152***	0.0162***	−0.527***	−0.220***	−0.0513***	−0.0371***	0.0488***	0.0251***	0.0730***	0.0625***	−0.0437***	0.0921
10 m	0.15	0.0109***	0.0300***	0.00910**	−0.576***	−0.114***	−0.0459***	−0.0468***	0.0274***	0.0546***	0.0833***	0.0793***	−0.0719***	0.0834
15 m	0.15	0.0355***	0.0225***	0.00199	−0.547***	−0.103***	−0.0376***	−0.0358***	−0.00286	0.0964***	0.0898***	0.0686***	−0.101***	0.075
60 m	0.15	0.0648***	0.0121	−0.00922	−0.442***	−0.0770***	−0.0767***	−0.0871***	−0.104***	0.117***	0.0812***	0.0308*	−0.319***	0.038
Daily	0.15	−0.0880	−0.147**	−0.0535	−0.200*	−0.0777	−0.0363	0.0860	−0.220**	0.324***	−0.00577	0.0582	−3.297***	0.0684
1 m	0.20	−0.0131***	0.00232***	0.00551***	−0.0554***	−0.483***	−0.125***	−0.0455***	0.0465***	0.0414***	−0.00605***	0.0157***	−0.0112***	0.0872
5 m	0.20	−0.0198***	0.0121***	0.0150***	−0.475***	−0.187***	−0.0398***	−0.0263***	0.000400	−0.000795	0.0565***	0.0516***	−0.0321***	0.0709
10 m	0.20	0.00159	0.0230***	0.0115***	−0.520***	−0.0950***	−0.0297***	−0.0306***	−0.0285***	0.0309***	0.0625***	0.0674***	−0.0550***	0.0665
15 m	0.20	0.0202***	0.0199***	0.00849**	−0.502***	−0.0794***	−0.0219***	−0.0203***	−0.0563***	0.0644***	0.0729***	0.0585***	−0.0775***	0.0592
60 m	0.20	0.0606***	0.0133	−0.00215	−0.401***	−0.0514***	−0.0717***	−0.0713***	−0.152***	0.108***	0.0707***	0.0334**	−0.238***	0.0305
Daily	0.20	−0.123**	−0.120**	−0.0549	−0.189**	−0.0625	−0.0240	0.0483	−0.301***	0.291***	−0.00585	0.0825	−2.729***	0.0622
1 m	0.25	−0.0168***	0.000218	0.00479***	−0.0420***	−0.431***	−0.109***	−0.0353***	0.0342***	−0.00190*	−0.0211***	0.00840***	−0.00873***	0.0609
5 m	0.25	−0.0230***	0.0102***	0.0119***	−0.426***	−0.160***	−0.0304***	−0.0178***	−0.0386***	−0.0184***	0.0437***	0.0409***	−0.0236***	0.0518
10 m	0.25	−0.000873	0.0202***	0.0110***	−0.476***	−0.0775***	−0.0203***	−0.0169***	−0.0782***	0.0151***	0.0512***	0.0532***	−0.0431***	0.0504
15 m	0.25	0.0169***	0.0185***	0.00883**	−0.467***	−0.0578***	−0.00880*	−0.0132**	−0.0979***	0.0403***	0.0639***	0.0490***	−0.0595***	0.0454
60 m	0.25	0.0581***	0.0158**	−0.00141	−0.371***	−0.0240*	−0.0558***	−0.0455***	−0.198***	0.0902***	0.0436***	0.0294**	−0.198***	0.0252
Daily	0.25	−0.101*	−0.102*	−0.0552	−0.175*	−0.0532	−0.0357	0.0128	−0.350***	0.301***	0.00896	0.107	−2.181***	0.0542
1 m	0.50	−0.0197***	−0.000372	0.00288***	−0.00458***	−0.196***	−0.0589***	−0.00715***	−0.000112	−0.203***	−0.0657***	−0.0117***	0.0000610	0.0011
5 m	0.50	−0.0250***	0.00674***	0.0119***	−0.216***	−0.0711***	0.00422*	0.00951***	−0.207***	−0.0918***	0.00410*	0.00995***	−0.000480	0.0055
10 m	0.50	−0.00297	0.0213***	0.0111***	−0.259***	−0.0162***	0.0125***	0.00378	−0.291***	−0.0431***	0.0134***	0.0215***	−0.00376***	0.0092
15 m	0.50	0.0133***	0.0179***	0.0187***	−0.262***	−0.000632	0.0205***	0.00418	−0.318***	−0.0222***	0.0221***	0.0209***	−0.00817***	0.0112
60 m	0.50	0.0581***	0.0249***	0.00194	−0.187***	0.0398***	−0.0240**	−0.00597	−0.409***	0.0332***	0.0204*	0.00789	−0.0476***	0.0163
Daily	0.50	−0.0456	−0.0296	0.0209	0.165*	−0.0675	−0.0731	−0.0795	−0.727***	0.187*	0.105	0.111	−0.444	0.0644
1 m	0.75	−0.0139***	0.00281***	0.00707***	0.0309***	0.00492***	−0.0141***	0.0114***	−0.0303***	−0.432***	−0.115***	−0.0368***	0.00903***	0.0656
5 m	0.75	−0.00483**	0.0172***	0.0171***	−0.0182***	0.00388	0.0417***	0.0394***	−0.432***	−0.190***	−0.0334***	−0.0217***	0.0173***	0.0571
10 m	0.75	0.0139***	0.0271***	0.0126***	−0.0263***	0.0543***	0.0352***	0.0333***	−0.517***	−0.124***	−0.0194***	−0.0106**	0.0263***	0.0647
15 m	0.75	0.0337***	0.0204***	0.0271***	−0.0207***	0.0549***	0.0476***	0.0237***	−0.546***	−0.0954***	−0.0202***	0.00129	0.0351***	0.0631
60 m	0.75	0.0815***	0.0259***	−0.00418	0.0680***	0.0957***	−0.00507	−0.00506	−0.642***	−0.0307**	0.0114	0.00271	0.0884***	0.0595
Daily	0.75	−0.000379	−0.0352	−0.0129	0.494***	−0.0495	−0.0129	−0.0426	−1.093***	0.280***	0.127	0.0576	0.832	0.1119
1 m	0.80	−0.00994***	0.00506***	0.00852***	0.0452***	0.0507***	−0.0000227	0.0204***	−0.0447***	−0.487***	−0.133***	−0.0466***	0.0110***	0.0953
5 m	0.80	0.000424	0.0210***	0.0200***	0.0312***	0.0267***	0.0534***	0.0507***	−0.488***	−0.225***	−0.0447***	−0.0298***	0.0228***	0.0814
10 m	0.80	0.0204***	0.0326***	0.0152***	0.0403***	0.0722***	0.0475***	0.0450***	−0.577***	−0.150***	−0.0276***	−0.0192***	0.0346***	0.0888
15 m	0.80	0.0391***	0.0238***	0.0299***	0.0527***	0.0768***	0.0555***	0.0316***	−0.601***	−0.127***	−0.0292***	−0.00635	0.0455***	0.0864
60 m	0.80	0.0864***	0.0314***	−0.00284	0.141***	0.116***	0.00206	−0.00456	−0.715***	−0.0649***	0.00748	−0.00688	0.118***	0.0747
Daily	0.80	0.0410	−0.0481	−0.0255	0.592***	0.0168	0.000268	−0.0332	−1.153***	0.308**	0.0892	0.0619	1.032	0.1205
1 m	0.85	−0.00569***	0.00783***	0.00967***	0.0632***	0.109***	0.0173***	0.0310***	−0.0621***	−0.553***	−0.154***	−0.0596***	0.0137***	0.1306
5 m	0.85	0.00919***	0.0273***	0.0229***	0.0860***	0.0608***	0.0697***	0.0638***	−0.554***	−0.268***	−0.0618***	−0.0442***	0.0296***	0.1104
10 m	0.85	0.0312***	0.0394***	0.0190***	0.118***	0.115***	0.0638***	0.0546***	−0.654***	−0.187***	−0.0423***	−0.0323***	0.0426***	0.1165
15 m	0.85	0.0537***	0.0288***	0.0325***	0.134***	0.103***	0.0782***	0.0466***	−0.670***	−0.156***	−0.0429***	−0.0203***	0.0570***	0.1122
60 m	0.85	0.0974***	0.0312***	0.00167	0.236***	0.165***	−0.00152	−0.00581	−0.821***	−0.0981***	0.000631	−0.000525	0.164***	0.0933

(*continued on next page*)

Table 7 (*continued*)

$$\Delta EVOL_{it} = \alpha^{(q)} + \sum_{L=1}^{3} \beta_L^{(q)} L\Delta EVOL_{it-L} + \sum_{L=0}^{3} \gamma_L^{+(q)} R_{it-L}^{+} + \sum_{L=0}^{3} \delta_L^{-(q)} R_{it-L}^{-} + u_t$$

	Quantile	$\Delta EVOL_{t-1}$	$\Delta EVOL_{t-2}$	$\Delta EVOL_{t-3}$	R_t^+	R_{t-1}^+	R_{t-2}^+	R_{t-3}^+	R_t^-	R_{t-1}^-	R_{t-2}^-	R_{t-3}^-	intercept	R^2
Daily	0.85	0.0708	−0.0145	−0.0466	0.674***	0.00989	0.0467	0.0301	−1.306***	0.394***	0.0150	0.0143	1.239	0.1448
1 m	0.90	−0.000128	0.0130***	0.0125***	0.0890***	0.176***	0.0438***	0.0457***	−0.0879***	−0.638***	−0.183***	−0.0730***	0.0189***	0.1712
5 m	0.90	0.0189***	0.0380***	0.0291***	0.152***	0.106***	0.103***	0.0855***	−0.651***	−0.332***	−0.0877***	−0.0638***	0.0399***	0.1451
10 m	0.90	0.0495***	0.0449***	0.0299***	0.203***	0.166***	0.0860***	0.0742***	−0.743***	−0.230***	−0.0595***	−0.0461***	0.0613***	0.1488
15 m	0.90	0.0392***	0.0375***	0.232***	0.159***	0.104***	0.0643***	−0.765***	−0.199***	−0.0655***	−0.0279***	0.0770***	0.0881***	0.1414
60 m	0.90	0.0301*	0.00601	0.391***	0.239***	0.0279	0.0131	−0.947***	−0.178***	−0.0174	−0.00214	0.202***	0.285***	0.1224
Daily	0.90	0.0416	−0.0309	−0.0592	0.837***	0.0983	−0.0607	−0.0381	−1.504***	0.320*	0.100	0.0613	2.258**	0.207
1 m	0.95	0.00892***	0.0222***	0.0156***	0.130***	0.269***	0.0914***	0.0793***	−0.137***	−0.765***	−0.241***	−0.102***	0.0312***	0.2156
5 m	0.95	0.0402***	0.0540***	0.0405***	0.264***	0.204***	0.171***	0.125***	−0.776***	−0.420***	−0.129***	−0.0921***	0.0669***	0.1885
10 m	0.95	0.0823***	0.0496***	0.0440***	0.365***	0.278***	0.125***	0.110***	−0.897***	−0.320***	−0.0836***	−0.0839***	0.0977***	0.1898
15 m	0.95	0.0990***	0.0488***	0.0393***	0.427***	0.262***	0.175***	0.104***	−0.910***	−0.289***	−0.0947***	−0.0577***	0.119***	0.1818
60 m	0.95	0.115***	0.0356	0.0188	0.631***	0.406***	0.0834**	0.0797**	−1.175***	−0.289***	−0.0154	−0.00621	0.294***	0.1782
Daily	0.95	−0.0111	0.00895	−0.0645	1.324***	0.245	0.229	−0.0270	−1.800***	0.203	0.100	0.0716	2.641	0.3333
1 m	OLS	0.0179	0.0198	−0.0178	0.0443	−0.225***	−0.0580***	−0.0461	−0.0386**	−0.258***	−0.0855***	−0.00888	−0.00439**	0.13738
5 m	OLS	−0.00419	0.0280	0.0178*	−0.203***	−0.0621*	0.00818	0.00522	−0.314***	−0.164***	0.0158	0.0232*	−0.0181***	0.0443
10 m	OLS	0.0354	0.0343***	0.0145*	−0.190***	0.0139	−0.00444	−0.0117	−0.365***	−0.121**	0.0387*	0.0370**	−0.0295***	0.0457
15 m	OLS	0.0405	0.0234*	0.0197	−0.177***	0.0165	0.00658	−0.00970	−0.442***	−0.0403*	0.0311*	0.0447**	−0.0405***	0.0505
60 m	OLS	0.0984***	0.0184	0.0000723	−0.0668*	0.0396*	−0.0513**	−0.0355	−0.581***	0.0413*	0.0222	0.0383	−0.118***	0.0757
Daily	OLS	−0.0424	−0.0484	−0.0152	0.359**	0.0542	0.0192	−0.0847	−0.983***	0.292***	0.0408	0.166*	−1.326*	0.222

Notes: This table provides findings from the lower to upper quantiles regression (0.05 to 0.95) and OLS regression for Ethereum. The results for all six time-intervals are grouped according to each q-value. R_t^+ and R_t^- represent the impact of contemporaneous positive and negative returns of Ethereum. R_{t-l}^+ and R_{t-l}^- represent the impact of lags of positive and negative returns of Ethereum. $\Delta EVOL_{t-1}$, $\Delta EVOL_{t-2}$ and $\Delta EVOL_{t-3}$ are the lags of the dependent variable (changes of EthVol). The significance level at 1 %, 5 % and 10 % are denoted by ***, ** and *, respectively.

The empirical findings reported in the above-mentioned tables and figures confirm that the return-volatility relationship of cryptocurrency has different asymmetries across the different volatility regimes—denoted by the changes of volatility at different quantiles—and, those asymmetries seem to be more pronounced at extreme tails of the distribution. However, those different asymmetries could not be captured by the OLS estimation, since it measures only the mean effects. It is also evident that the contemporaneous returns seem to be more imperative in determining the changes of the volatility than the lagged returns.

The absolute difference in the impact of positive and negative contemporaneous returns of Bitcoin (Ethereum) is presented in the upper-left (upper-right) panel of Fig. 3 as a dashed line with a small square-shaped curve. The findings show that the asymmetry is more visible (less visible) at lower quantiles (higher quantiles) of the volatility distributions. Specifically, the asymmetry was observed to reduce as we move from the lowermost (q = 0.05) to the second-last quantiles (q = 0.90) of the distribution. The magnitude of the coefficients of positive contemporaneous returns seems to be higher than that of negative contemporaneous returns at lower to medium quantiles (q = 0.05 to 0.5). Although the absolute values of the coefficients of positive and negative returns were slowly converging as we move from medium to upper quantiles, the size of the negative coefficients was slightly bigger. This indicates that, for intraday data frequency, the asymmetry is more pronounced at the lower quantiles of the volatility distributions. The marginal effect of positive (negative) returns is(slightly) higher at lower (upper) quantiles. Therefore, the findings demostrate that a positive asymmetry exists at lower to medium quantiles of the volatility distribution, while the negative asymmetry that exists at upper quantiles of the volatility distribution is less visible using the intraday data.

We present the results using the daily data interval in Table 3 (Table 5) for Bitcoin (Ethereum). In addition, the effects of contemporaneous positive and negative returns along with their absolute differences were plotted for Bitcoin in the lower-left panel and Ethereum in the lower-right panel of Fig. 3. There are a few major differences in estimated results for 1-min and daily data intervals. First, the magnitude of the estimated coefficients is higher for the daily data interval. As a result, the return-volatility relationship is more pronounced at the daily data interval than at the intraday data interval. Second, the size of the absolute differences between positive and negative return coefficients is bigger for daily data intervals. Accordingly, the asymmetry of the return-volatility relationship was higher for the daily data interval than the 1-min data interval across all quantiles. However, unlike the results of the 1-min interval, the autocorrelation (with the lags of changes of the volatility) and cross-autocorrelation (with the lags of positive and negative returns) at the daily data interval are almost insignificant for most of the cases—except for the first lag of negative returns. This implies that the impact of the past returns on the changes of volatility is more persistent at high-frequency trading; whereas, at daily trading, only negative past returns tend to have a significant and less persistent impact on the volatility changes. Moreover, unlike the coefficients of positive returns, the coefficients of contemporaneous negative returns are significant across the quantiles. This suggests that the effect of contemporaneous negative return shocks on volatility is persistent across the quantities at both daily and intraday levels, whereas the effect of positive contemporaneous return shock is persistent for intraday data but not for the daily data (only persistent at medium to high volatility regimes).

During the medium to high volatility regimes, both positive and negative return shocks are positively associated with the changes in volatility. This finding is the same for both 1-min and daily data intervals and also for both Bitcoin and Ethereum. This observation constitutes the major similarities in estimated results for 1-min and daily data intervals and also supports the finding of Baur et al. (2018), who found that both positive and negative returns are linked to an increase—a positive innovation—in the cryptocurrency volatility.

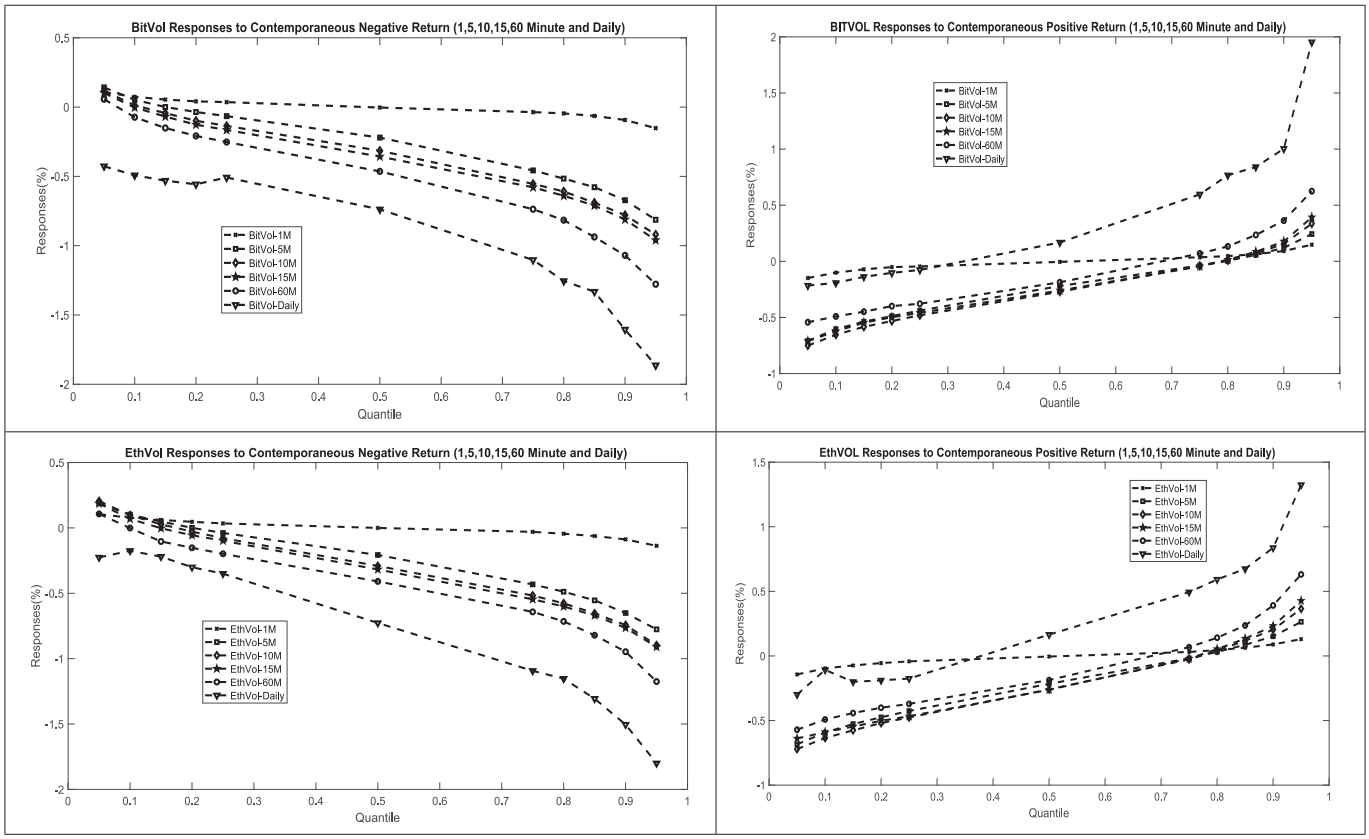

Fig. 4. QRM Estimates Across Quantiles: Response Variables Δ*EthVol* and Δ*BitVol* at 1, 5, 10, 15, 60 min and Daily.

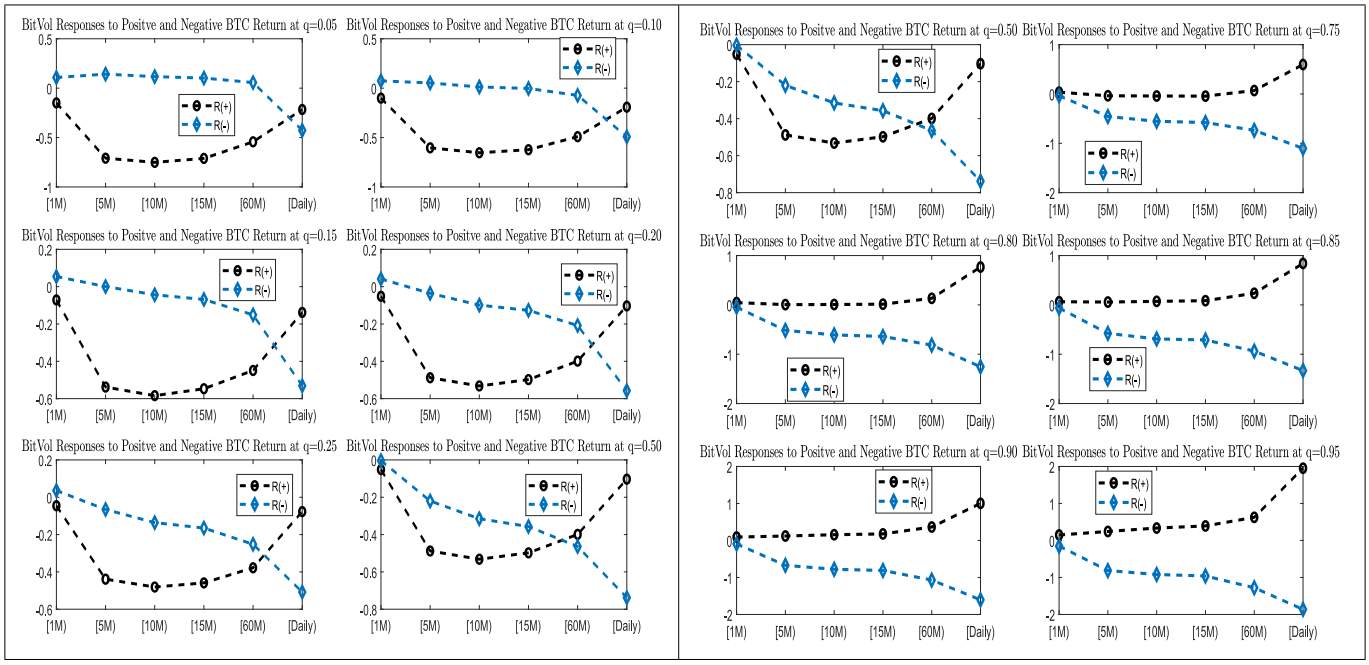

Fig. 5. QRM Estimates: Δ*BitVol* Response Comparison Across Time Intervals (1,5,10,15, 60 min and day) at Each Quantile.

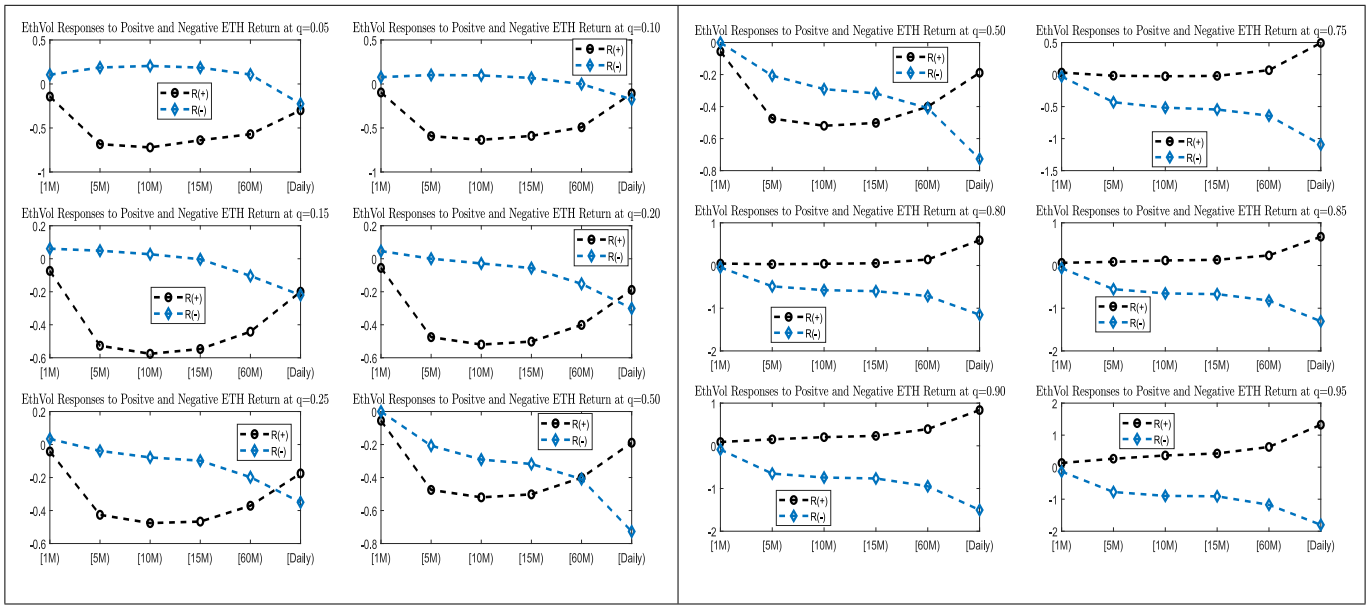

Fig. 6. QRM Estimates: Δ*EthVol* Response Comparison Across Time Intervals (1,5, 10, 15, 60 min and day) at Each Quantile.

Furthermore, using the daily data, a positive return shock tends to create a greater response to cryptocurrency volatility, compared to a negative return shock. This suggests that good news tends to have more impact on cryptocurrency volatility than bad news. This positive asymmetric (inverted asymmetric) reaction can be attributed to the noise trading activity, as indicated by Baur et al. (2018) and Cheikh et al. (2020). Our paper also corrobotes with the findings Wang and Ngene (2020), who observed that Bitcoin processes more predictive power about future price movement and transmission of volatility and returns in both bull and bear market environments. Leirvik (2022) also observed a time-varying positive relationship between the liquidity volatility and returns of the largest five cryptocurrencies including Bitcoin and Ethereum.

4.2. Comparisons of the intraday asymmetric return-volatility relations across sampling frequency

For the robustness assessment, we report the results for the QRM estimates of model (5) in Tables 6 and 7 for Bitcoin and Ethereum, respectively. The results for all six time intervals were grouped according to each q-value. Also, the estimates of the OLS in Model 4 are reported in the last six rows of Tables 6 and 7. Additionally, the impact of contemporaneous positive and negative returns on the changes of their respective volatility are also presented in Fig. 4 over different intraday return horizons (i.e., 1, 5, 10, 15, 60-min and daily) and quantiles (i.e., q = 0.05…to 0.95). The positive and negative returns covariates were plotted against different quantiles for all six intraday time intervals. The x-axis shows the 11 quantile parameters (q = 0.05… to 0.95), while the y-axis shows the estimated effect as a percentage. The upper-left (upper-right) panel of Fig. 4 plots the responses of the changes of BitVol to the contemporaneous negative (positive) return of Bitcoin. In addition, the lower-left (lower-right) panel of Fig. 4 plots the responses of the changes of EthVol to the contemporaneous negative (positive) return of Ethereum.

Accordingly, we compare the short-term asymmetric return-volatility relations over different intraday return horizons, and observe the following. First, across the conditional distribution of the volatility changes, the result show that the return-volatility relationship is asymmetric. Particularly, the asymmetry is high (low) at lower (higher) frequency data. Furthermore, using low (high) frequency data, asymmetry is more visible at upper (lower) quantiles of the volatility distribution. Second, the results indicated that the response to *negative* (*positive*) returns is a monotonically *decreasing* (*increasing*) function of the return horizons and more pronounced at medium to uppermost quantiles of the volatility distributions (during medium to high volatility regimes). Third, the absolute values of the coefficients keep increasing as we move from the highest frequency of the data to the lowest frequency of the data (i.e.: Daily >60 m > 15 m > 10 m > 5 m > 1 m), thus confirming that the changes of the volatility are more sensitive in the daily data than in the intraday data frequencies. Moreover, the absolute values of the coefficients also keep increasing as we move from the lowest quantiles (q = 0.05) to the highest quantile (q = 0.95) of the volatility distributions, thereby validating that the return-volatility relationship is more pronounced during the medium to high volatility regimes.

For further investigation, in Fig. 5 (Bitcoin) and Fig. 6 (Ethereum), the responses to positive and negative returns were plotted against the six time intervals (i.e., 1, 5, 10, 15, 60-min and daily) for each quantile (i.e., q = 0.05 to 0.95) separately. For the high-frequency return horizons (i.e., 1 m, 5 m, 10 m, 15 m, 60 m), the asymmetry—denoted by the vertical distance between positive and negative lines in Figs. 5 and 6—is a decreasing function of the size of the time interval. Hence, the vertical distance narrowed down to the lowest at 60 m return horizons for the quantiles below the median ($q \leq 0.5$). In contrast, the asymmetry is an increasing function of the return horizons for the quantiles above the median ($q > 0.5$). Moreover, the results showed that the asymmetry is more pronounced at the daily return horizon, especially at medium to high quantiles.

Our findings add to the previous papers by Naeem et al. (2023), Zhang and Zhao (2023), Wang et al. (2024), among others, who analyze the relationships between cryptocurrencies and other assets using approaches capable of capturing the asymmetry in connectedness.

5. Robustness test

For robustness checking, we divided the full sample data at a 1-min frequency into two equal sub-samples for both cryptocurrencies. To be consistent with quantile regression analysis, we first divided the data into quantiles ranging from the lowest to the highest of the distribution

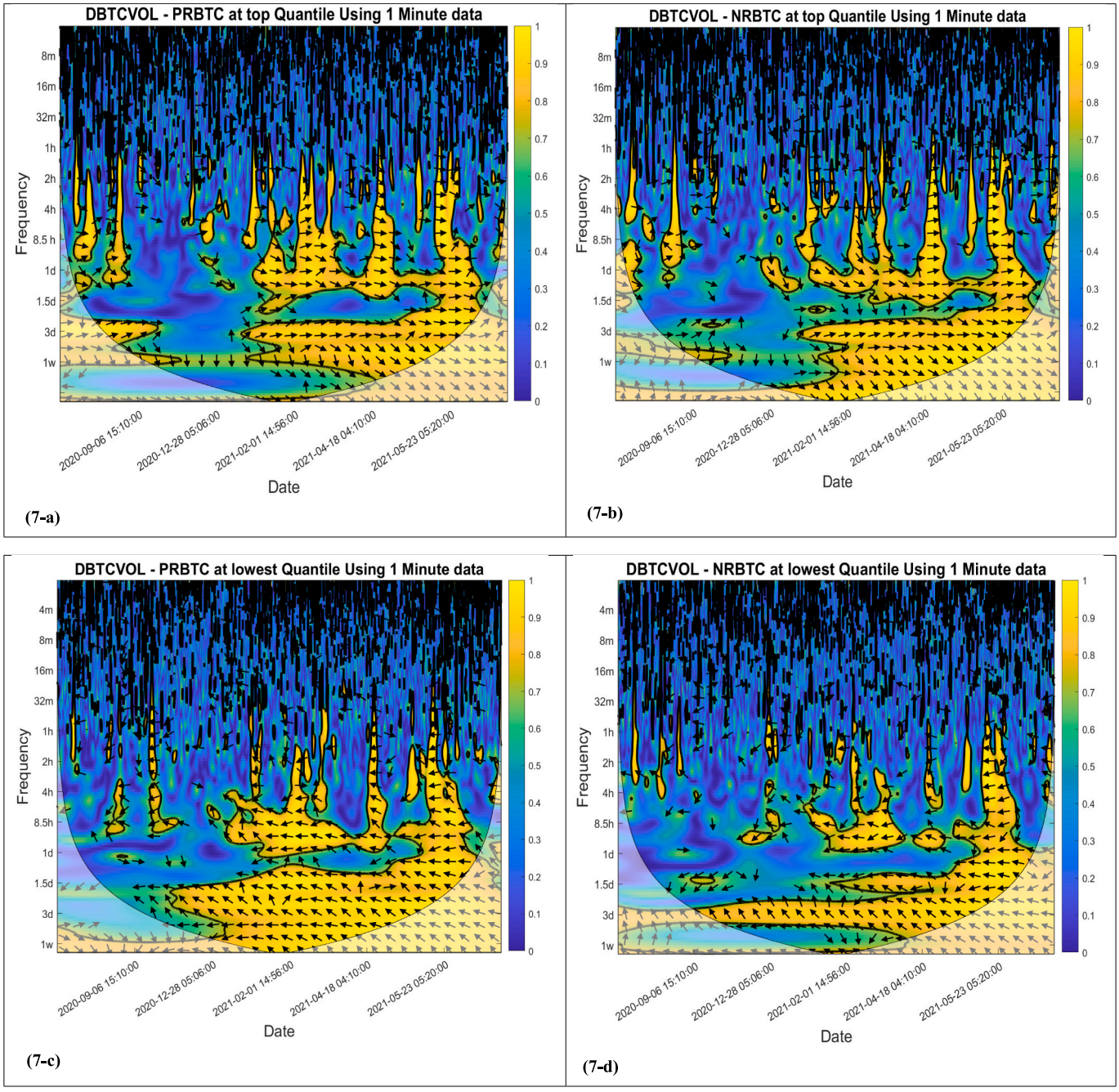

Fig. 7. Wavelet Coherence between Changes of BitVol (DBTCVOL), Positive Return (PRBTC), and Negative Return (NRBTC) of Bitcoin.
Note: DBTCVOL refers to changes of Bitcoin Implied Volatility (ΔBitVol), PRBTC refers to positive returns of Bitcoin (R_t^+), and NRBTC refers to negative returns of Bitcoin (R_t^-).

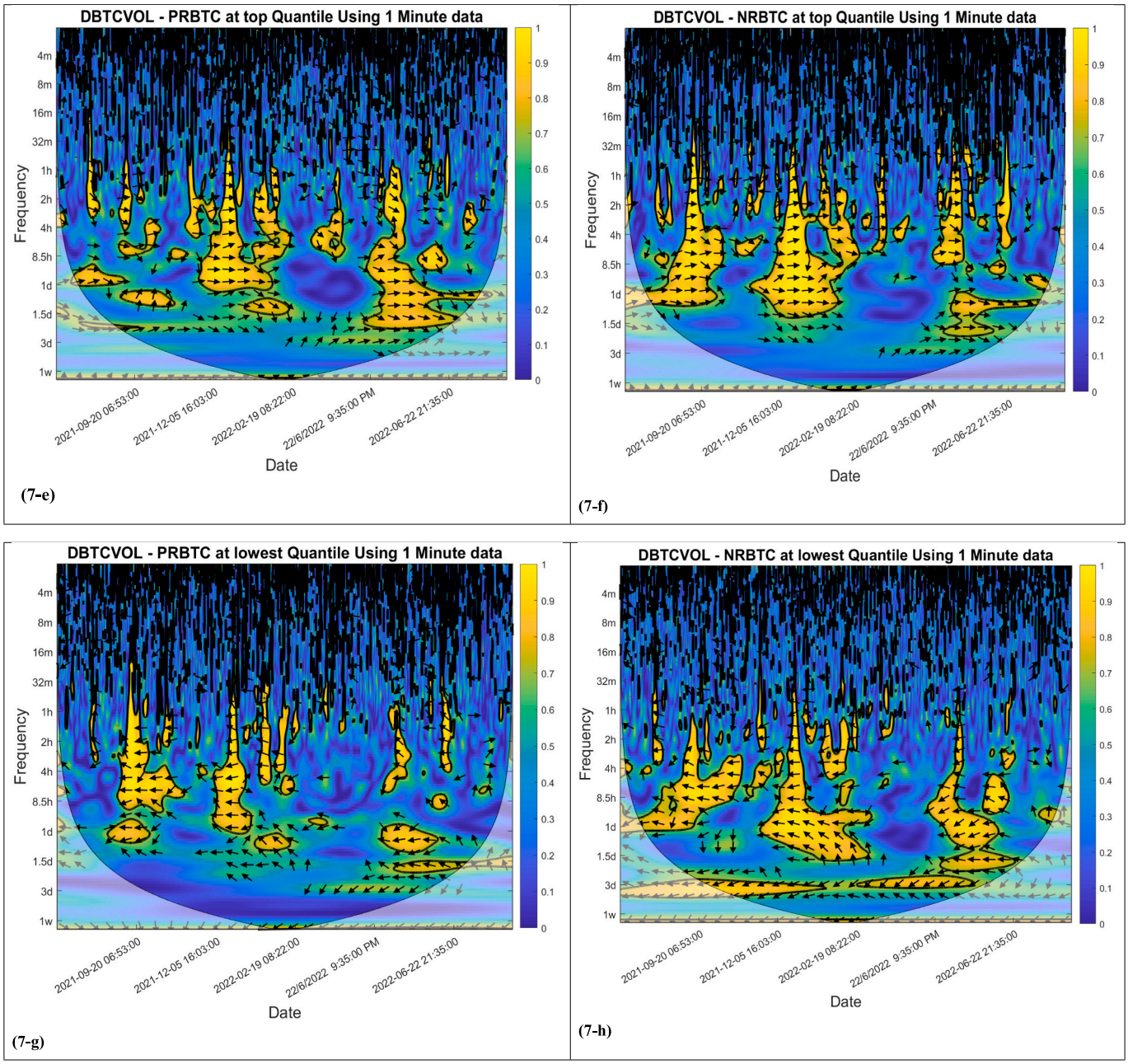

Fig. 7. (*continued*).

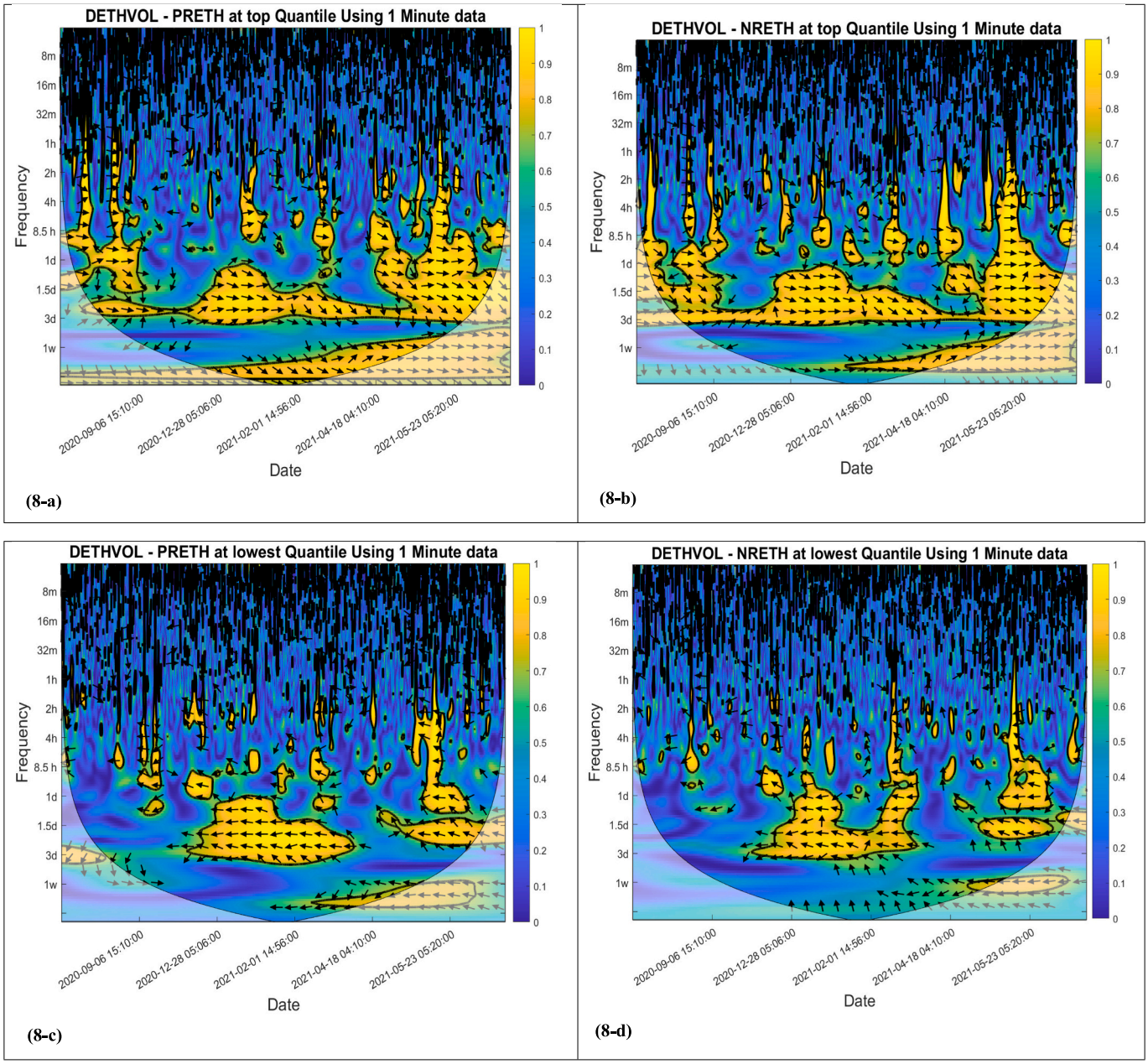

Fig. 8. Wavelet Coherence between Changes of EthVol (DETHVOL), Positive Return (PRETH), and Negative Return (NRETH) of Ethereum.
Note: DETHVOL refers to changes of Ethereum Implied Volatility (ΔEthVol), PRETH refers to positive returns of Ethereum (R_t^+), and NRETH refers to negative returns of Ethereum (R_t^-).

of the implied volatilities for each cryptocurrency before running wavelet coherence. Due to page limitations, we present only the results for the lowest and highest quantiles in this paper.

Figs. 7a-7d (7e-7 h) depict wavelet coherences between changes in Bitcoin's implied volatility and its positive and negative returns using the first (second) sub-sample of the data. Moreover, Figs. 8a-8d (8e-8 h) illustrate wavelet coherences between changes in Ethereum's implied volatility and its positive and negative returns using the first (second) sub-sample of the data. The x-axis of the aforementioned figures represents the time domain, indicating the time span covered by the data. The y-axis represents the frequency domain, indicating the range of frequencies analyzed in the wavelet coherence analysis (i.e., 4 min to 1 week). The color of the ruler indicates the level of coherence. The arrow indicates a direction (positive or negative) and lead-lag relationship between the variables.

If the arrow points to the right, it indicates a positive or in-phase relationship between the volatility and returns. Conversely, when the arrow points to the left, it suggests a negative or anti-phase relationship between the volatility and returns. Regarding causality, if the arrow points downward and to the right or upward and to the left, it implies that return causes the volatility. Conversely, if the arrow points downward and to the left or upward and to the right, it suggests that volatility causes the return.

The insights derived from Fig. 7c, d, g, and h, as well as Fig. 8c, d, g, and h, offer a detailed portrayal of the nuanced relationship between cryptocurrency volatility and returns across different volatility regimes. Specifically, these figures illuminate distinct patterns observed during low and high volatility regimes, as delineated by quantiles of the volatility distribution. During periods of low volatility, characterized by the lowest quantile of the volatility distribution, changes in Bitcoin's (or

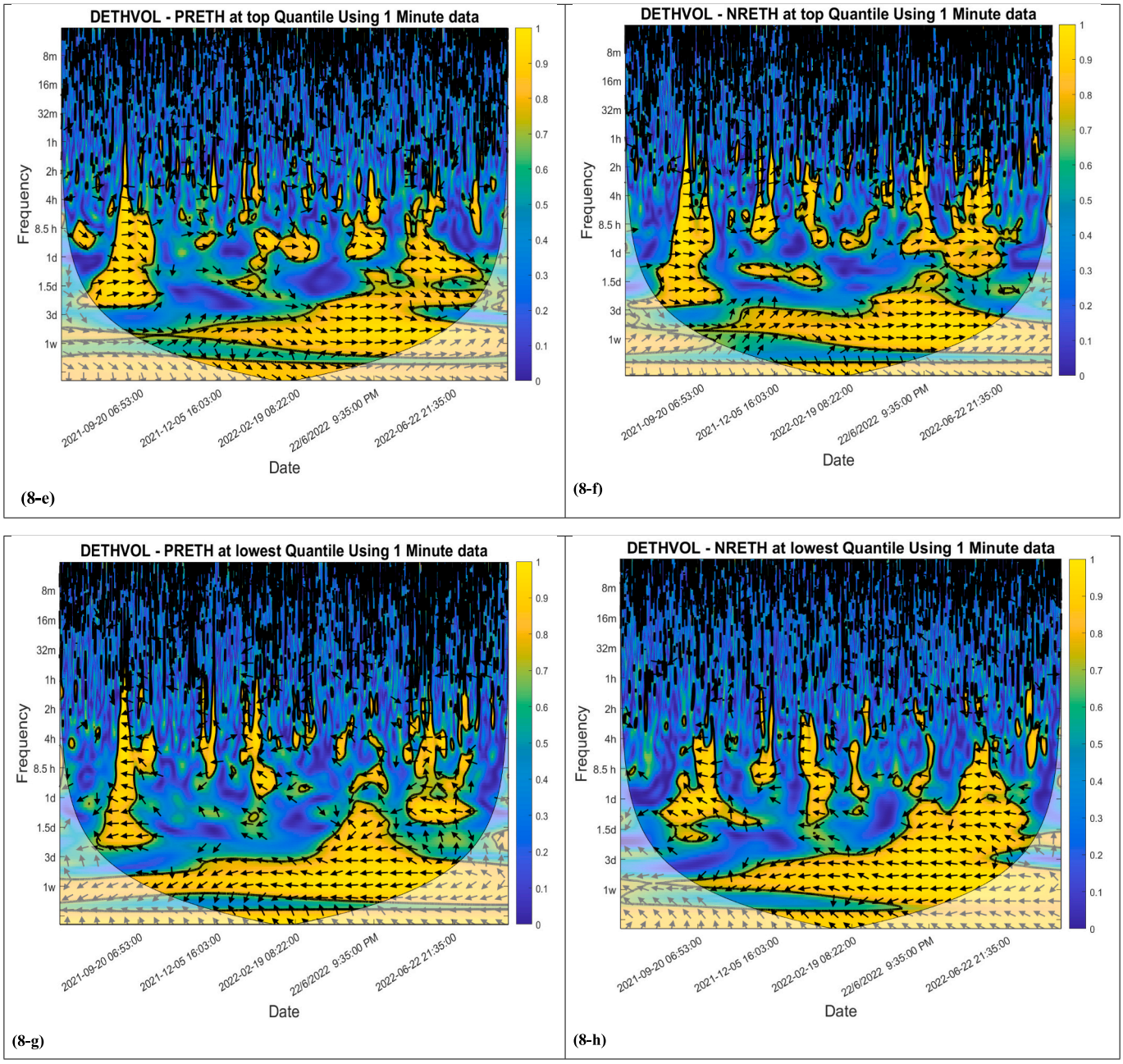

Fig. 8. (*continued*).

Ethereum's) implied volatility exhibit a negative association with both positive and negative returns of the respective cryptocurrency, as depicted in Fig. 7c, d, g, and h (as well as Fig. 8c, d, g, and h). Conversely, during high volatility regimes, represented by the highest quantile of the volatility distribution, Fig. 7e, f, g, and h (as well as Fig. 8e, f, g, and h) illustrate a positive relationship between cryptocurrency volatility (BitVol and EthVol) and the corresponding positive and negative returns. Notably, the impact of positive and negative returns on volatility changes is accentuated at the extreme tails of the volatility distributions, as observed in the highest quantile. This heightened sensitivity underscores the significance of extreme market conditions in influencing the dynamics of cryptocurrency volatility, with the potential for amplified reactions to market shocks and fluctuations.

The findings presented in the aforementioned figures offer compelling insights into the nature of the return-volatility relationship in cryptocurrency markets, particularly in relation to different data frequencies. Notably, the figures reveal that the return-volatility relationship exhibits greater prominence and clarity at lower-frequency data intervals, such as daily, three-day, and weekly intervals, as indicated by the pronounced coherence levels on the y-axis denoted by 1d, 3d, and 1w. In contrast, at intraday data intervals, including 4-min, 8-min, and 16-min intervals denoted by 4 m, 8 m, and 16 m on the y-axis, the observed return-volatility relationship appears to be comparatively less pronounced. This distinction suggests that the dynamics driving the return-volatility relationship may vary depending on the time horizon considered, with longer-term trends potentially exerting a more

significant influence on volatility compared to shorter-term fluctuations. Furthermore, the dynamic nature of the return-volatility relationship underscores its responsiveness to changes in market conditions and volatility regimes, highlighting the complexity inherent in cryptocurrency markets. These findings are notably consistent with the results obtained from quantile regression models discussed in an earlier section, further corroborating the robustness and reliability of the observed relationships across different analytical approaches. Overall, the nuanced insights from these analyses deepen our understanding of the dynamics underlying cryptocurrency markets and underscore the importance of considering both temporal and frequency factors when evaluating their behavior.

Figs. 7a-7d, focusing on Bitcoin, provide compelling insights into the dynamics of the return-volatility relationship amid the evolving phases of the Covid-19 pandemic. Specifically, these figures shed light on how the strength of this relationship varied between different stages of the pandemic. During the initial phase of the pandemic, encapsulated by the first sub-sample of the data, the observed return-volatility relationship exhibited a notably higher intensity. This heightened relationship underscores the heightened market turbulence and uncertainty characterizing the early stages of the pandemic, where rapid shifts in investor sentiment and market conditions likely led to increased volatility in Bitcoin market. In contrast, the subsequent stages of the Covid-19 pandemic, as depicted in Figs. 7e-7h, portray a moderation in the intensity of the return-volatility relationship. This observation suggests a potential stabilization or adaptation of market dynamics as participants adjusted to the prolonged effects of the pandemic. By delineating these temporal variations in the return-volatility relationship, the figures offer valuable insights into the evolving nature of market dynamics amidst significant external shocks, such as the Covid-19 pandemic, thus providing a better understanding of cryptocurrency market behavior over time.

Our findings are consistent with the findings of Corbet and Katsiampa (2020) who observed asymmetric reverting patterns of Bitcoin price returns, and higher persistency of positive price returns over the negative price returns in different time frequencies such as minute, hour, day and week.

6. Conclusion

Our study sheds light on the nuanced return-volatility dynamics in the cryptocurrency market, challenging traditional perspectives and providing valuable insights for investors and policymakers. The asymmetry information hypothesis holds true even in the realm of high-frequency data, revealing that both positive and negative returns exert comparable impacts on volatility, diverging from conventional wisdom in traditional asset classes. Notably, this asymmetry is not uniform across volatility regimes, adding a new layer of complexity to understanding cryptocurrency behavior. Our results build on previous findings reported by Baur et al. (2018), Cheikh et al. (2020), Kakinaka and Umeno (2022), Yarovaya and Zieba (2022), Katsiampa et al. (2022), and Karim et al. (2023) by providing novel evidence using MFIV indices and 1, 5, 10, 15, and 60-min data. Our granular data uncover nuanced aspects of the return-volatility relationship that might be obscured when utilizing lower-frequency data. By harnessing the power of high-frequency data analysis, we gain deeper insights into the underlying dynamics of the Bitcoin and Ethereum markets, shedding light on their behavior across varying levels of market activity and volatility.

These findings exert significant implications for the foundations of financial theory. Cryptocurrencies, as a disruptive asset class, defy conventional investment norms, indicating a shift away from rational expectations theory. Our results underscore the growing influence of irrationality in investor decision-making, where price changes, rather than their direction, become the primary random element. Positive news holds heightened significance, triggering investor scrutiny and drawing attention beyond the typical investment audience. The euphoria surrounding rising prices introduces an element of unpredictability, challenging established norms.

Practically, these insights reflect the sentiments of informed investors, acknowledging the difficulty in comprehending extreme volatility and price fluctuations. The observed patterns may potentially destabilize the overall crypto market, raising questions about the true nature and purpose of cryptocurrencies. While our findings resist easy categorization under a single theory, they necessitate an adaptation of conventional financial wisdom to account for the evolving dynamics of investment behavior. As the market continues to demonstrate unconventional patterns, the understanding of cryptocurrencies and their role in the financial landscape remains intriguing, inviting further research and policy considerations to navigate this unique and dynamic asset class.

For future research endeavors, delving into the factors that influence the relationship between cryptocurrency returns and volatility promises to yield valuable insights. While this study focused on cryptocurrencies with available implied volatilities, namely BITVOL for Bitcoin and ETHVOL for Ethereum, there remains a vast array of digital assets whose implied volatilities are yet to be explored. As the cryptocurrency landscape continues to evolve, it would be intriguing to expand these investigations to include a broader spectrum of cryptocurrencies once their implied volatilities become accessible. By incorporating additional cryptocurrencies into the analysis, future studies can provide a more comprehensive understanding of the complex interplay between returns and volatility across various digital assets, potentially uncovering novel factors that shape market dynamics and investor behavior in the crypto space.

Disclosure statement

The authors report there are no competing interests to declare.

Data availability

The data that support the findings of this study are available on request from the authors.

Acknowledgements

We are thankful to Mr. Simon Ho and Mr. Alexadr Sergeevich from the T3-index for providing us with the intraday (15-s interval) data for this study. Furthermore, we would like to acknowledge that this research submission fee has been funded by the University of Southampton Malaysia (UoSM) Journal Submission Fund (Project Code: UoSM/JSF2024/01).

Appendix A. Appendix

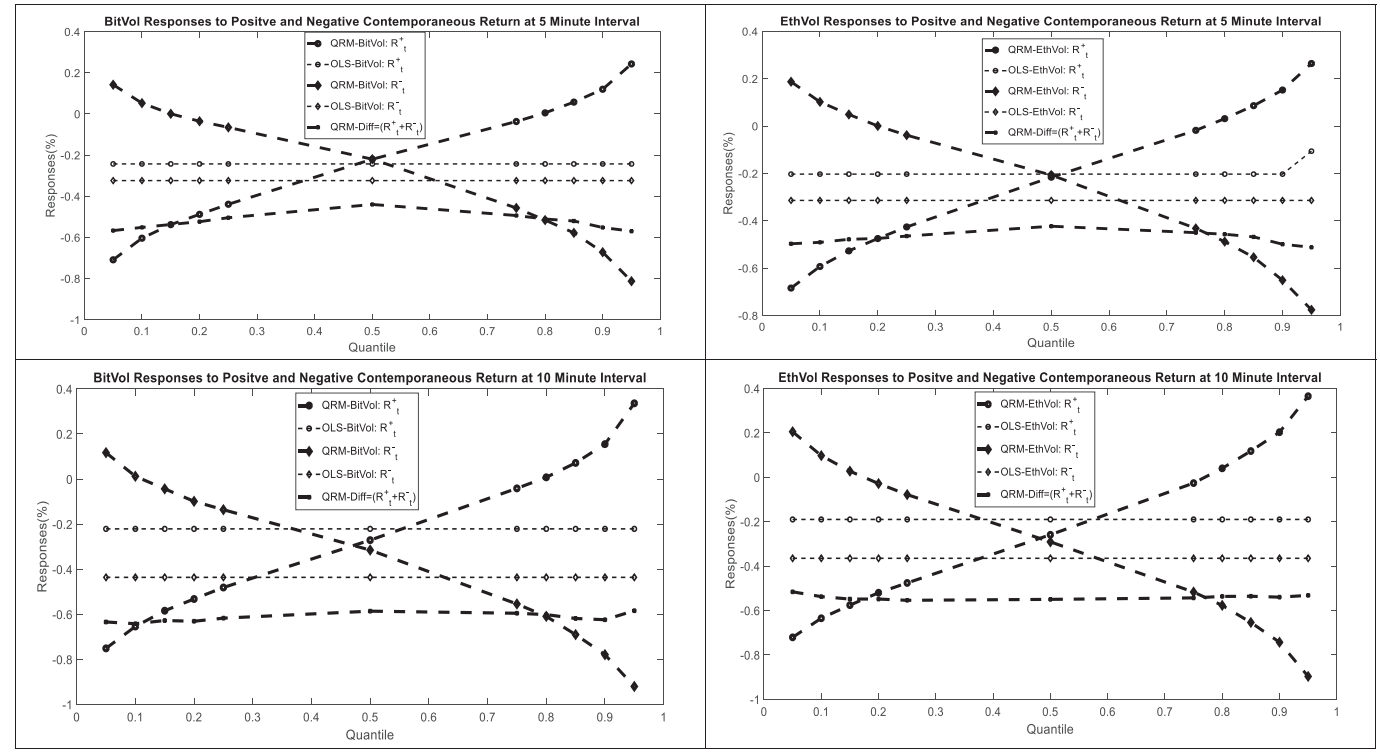

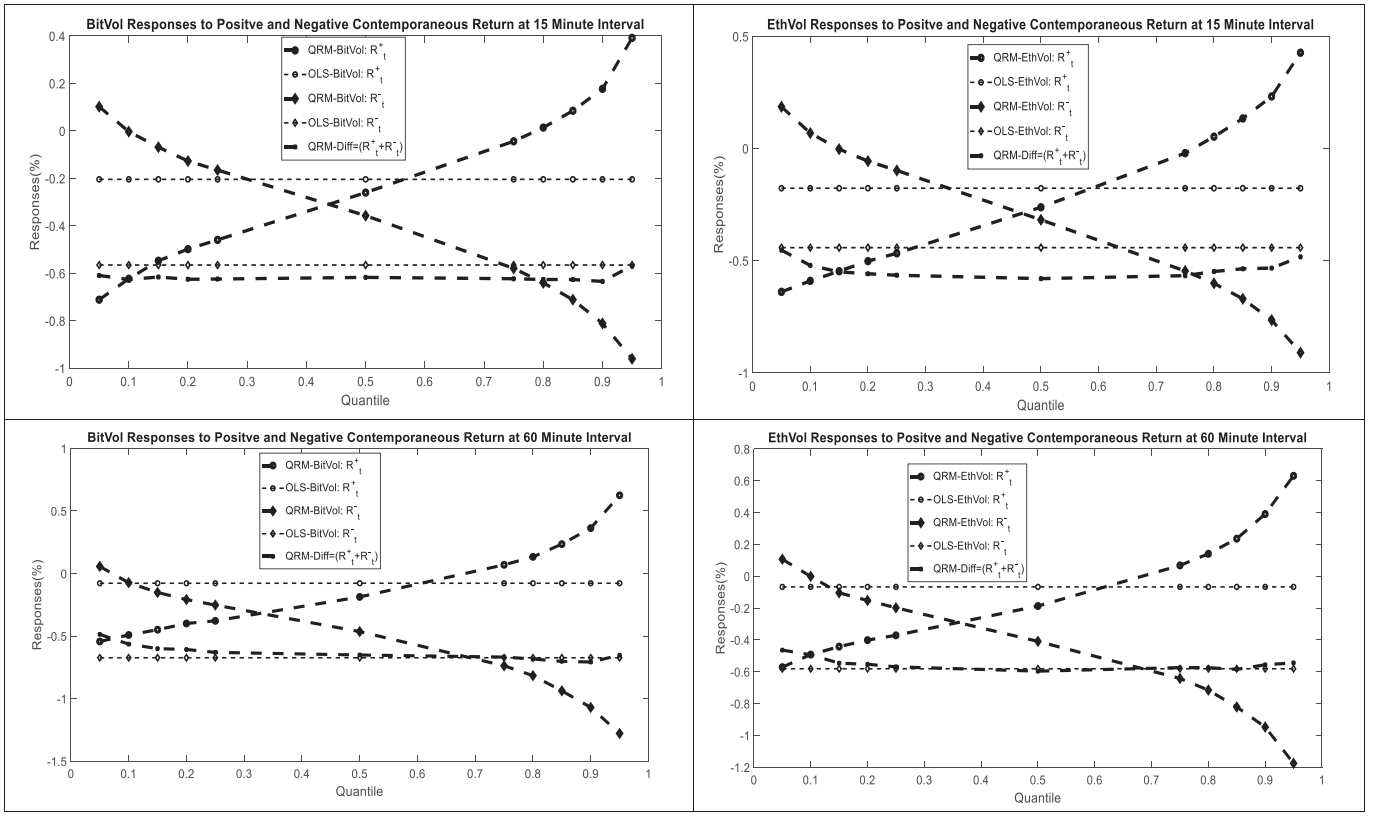

Fig. 9. Asymmetric Responses of Δ*EthVol* and Δ*BitVol* to Positive and Negative Returns of Bitcoin and Ethereum.

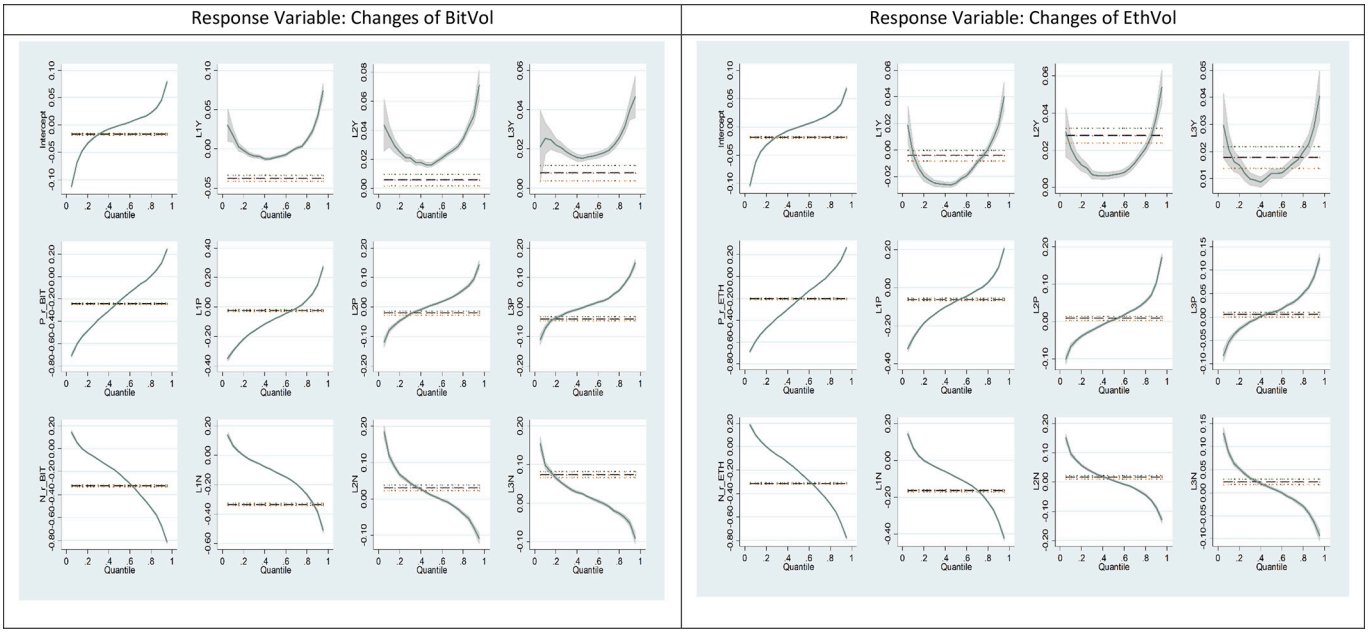

Fig. 10. QRM Plots - Using 5-Minute Data.
P_r_BIT is the positive contemporaneous returns of Bitcoin, **P_r_ETH** is the positive contemporaneous returns of Ethereum, **L1p to L3P** are the lags of the positive returns, **N_r_BIT** is the negative contemporaneous returns of Bitcoin, **N_r_ETH** is the negative contemporaneous returns of Ethereum, and **L1N to L3N** are the lags of the negative returns.

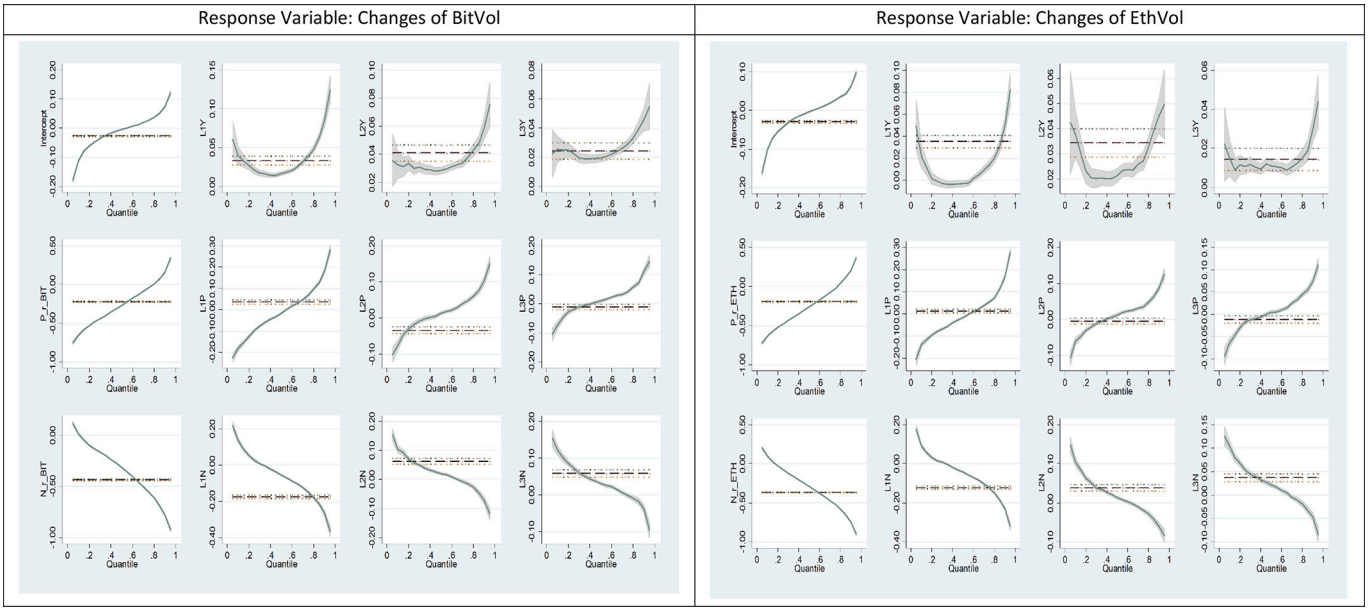

Fig. 11. QRM Plots Using 10-Minute Data.
P_r_BIT is the positive contemporaneous returns of Bitcoin, **P_r_ETH** is the positive contemporaneous returns of Ethereum, **L1p to L3P** are the lags of the positive returns, **N_r_BIT** is the negative contemporaneous returns of Bitcoin, **N_r_ETH** is the negative contemporaneous returns of Ethereum, and **L1N to L3N** are the lags of the negative returns.

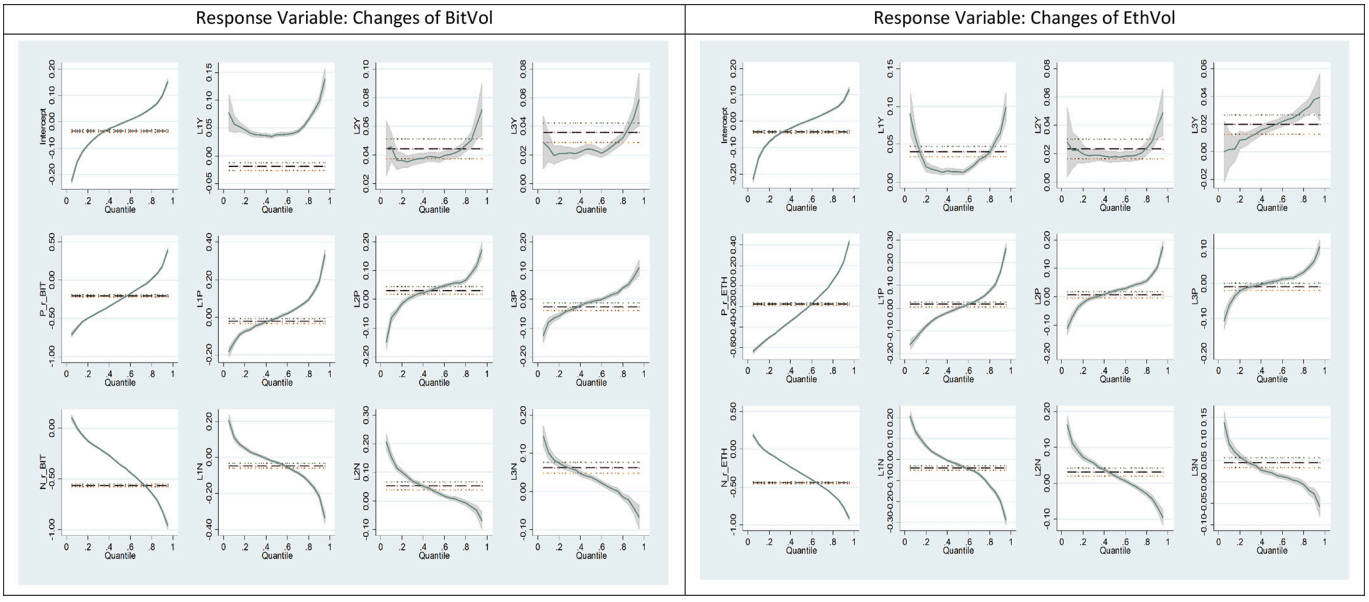

Fig. 12. QRM Plots Using 15-Minute Data.
P_r_BIT is the positive contemporaneous returns of Bitcoin, **P_r_ETH** is the positive contemporaneous returns of Ethereum, **L1p to L3P** are the lags of the positive returns, **N_r_BIT** is the negative contemporaneous returns of Bitcoin, **N_r_ETH** is the negative contemporaneous returns of Ethereum, and **L1N to L3N** are the lags of the negative returns.

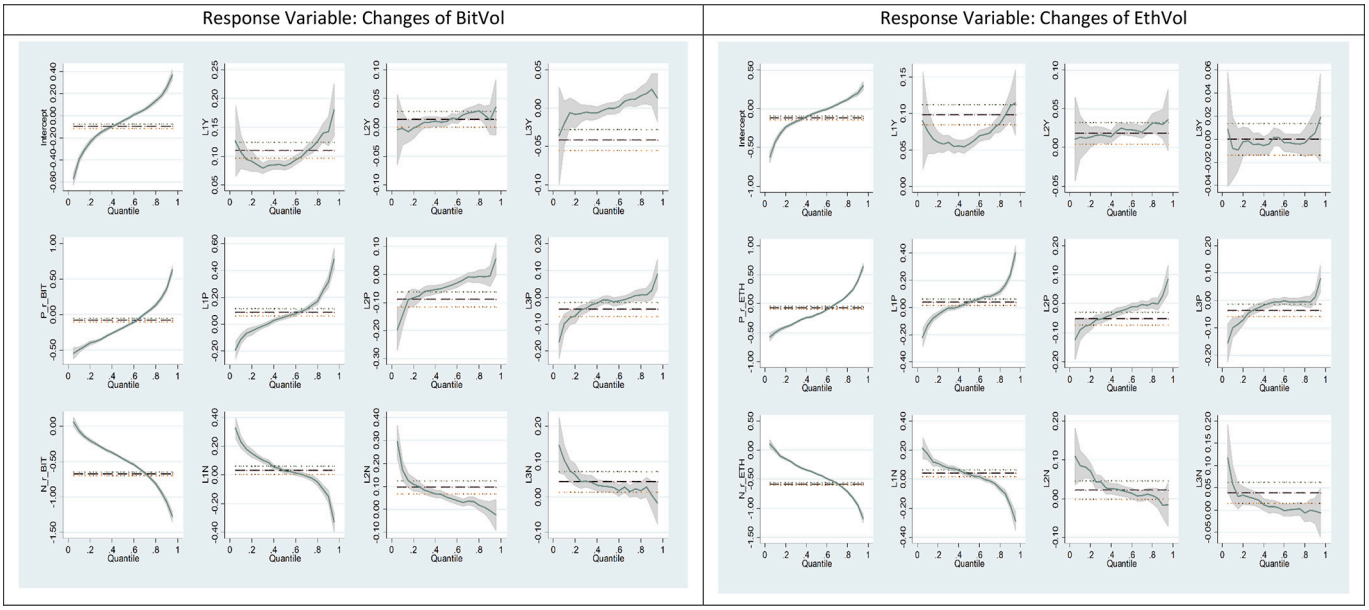

Fig. 13. QRM Plots Using 60-Minute Data.
P_r_BIT is the positive contemporaneous returns of Bitcoin, **P_r_ETH** is the positive contemporaneous returns of Ethereum, **L1p to L3P** are the lags of the positive returns, **N_r_BIT** is the negative contemporaneous returns of Bitcoin, **N_r_ETH** is the negative contemporaneous returns of Ethereum, and **L1N to L3N** are the lags of the negative returns.

References

Aguilera, R. F., & Radetzki, M. (2017). The synchronized and exceptional price performance of oil and gold: Explanations and prospects. *Resources Policy, 54*, 81–87.

Aït-Sahalia, Y., & Xiu, D. (2019). A Hausman test for the presence of market microstructure noise in high-frequency data. *Journal of Econometrics, 211*(1), 176–205.

Badshah, I., Frijns, B., Knif, J., & Tourani-Rad, A. (2016). Asymmetries of the intraday return-volatility relation. *International Review of Financial Analysis, 48*, 182–192.

Badshah, I. U. (2013). Quantile regression analysis of the asymmetric return-volatility relation. *Journal of Futures Markets, 33*(3), 235–265.

Baek, C., & Elbeck, M. (2015). Bitcoins as an investment or speculative vehicle? A first look. *Applied Economics Letters, 22*(1), 30–34.

Ballis, A., & Drakos, K. (2020). Testing for herding in the cryptocurrency market. *Finance Research Letters, 33*, Article 101210.

Banerjee, A. K. (2021). Futures market and the contagion effect of COVID-19 syndrome. *Finance Research Letters, 43*, Article 102018.

Banerjee, A. K., Akhtaruzzaman, M., Dionisio, A., Almeida, D., & Sensoy, A. (2022). Nonlinear nexus between cryptocurrency returns and COVID-19 news sentiment. *Journal of Behavioral and Experimental Finance, 36*, 100747.

Bariviera, A. F. (2017). The inefficiency of bitcoin revisited: A dynamic approach. *Economics Letters, 161*, 1–4.

Baur, D. G., & Dimpfl, T. (2018). Asymmetric volatility in cryptocurrencies. *Economics Letters, 173*, 148–151.

Baur, D. G., Hong, K., & Lee, A. D. (2018). Bitcoin: Medium of exchange or speculative assets? *Journal of International Financial Markets Institutions and Money, 54*, 177–189.

Bekaaert, G., & Wu, G. (2000). Asymmetric volatility and risk in equity markets. *The Review of Financial Studies, 13*(1), 1–42.

Bibinger, M., & Winkelmann, L. (2015). Econometrics of co-jumps in high-frequency data with noise. *Journal of Econometrics, 184*(2), 361–378.
Black, F. (1976). Studies of stock market volatility changes. In *1976 proceedings of the American Statistical Association business and economic statistics section*.
Bloomfield, J., Polman, R., & O'Donoghue, P. (2004). The 'Bloomfield movement classification': Motion analysis of individual players in dynamic movement sports. *International Journal of Performance Analysis in Sport, 4*(2), 20–31.
Bouri, E., Azzi, G., & Dyhrberg, A. H. (2017). On the return-volatility relationship in the bitcoin market around the price crash of 2013. *Economics, 11*(1).
Bouri, E., Gil-Alana, L. A., Gupta, R., & Roubaud, D. (2018). Modelling long memory volatility in the bitcoin market: Evidence of persistence and structural breaks. *International Journal of Finance and Economics, 24*(1), 412–426. https://doi.org/10.1002/ijfe.1670
Bouri, E., Gupta, R., & Roubaud, D. (2019). Herding behaviour in cryptocurrencies. *Finance Research Letters, 29*, 216–221.
Buchinsky, M. (1998). Recent advances in quantile regression models: A practical guideline for empirical research. *Journal of Human Resources*, 88–126.
Campbell, J. Y., & Hentschel, L. (1992). No news is good news: An asymmetric model of changing volatility in stock returns. *Journal of Financial Economics, 31*(3), 281–318.
Chaim, P., & Laurini, M. P. (2018). Volatility and return jumps in bitcoin. *Economics Letters, 173*, 158–163.
Charles, A., & Darné, O. (2019). Volatility estimation for bitcoin: Replication and robustness. *International Economics, 157*, 23–32.
Cheikh, N. B., Zaied, Y. B., & Chevallier, J. (2020). Asymmetric volatility in cryptocurrency markets: New evidence from smooth transition GARCH models. *Finance Research Letters, 35*, Article 101293.
Christie, A. A. (1982). The stochastic behavior of common stock variances: Value, leverage and interest rate effects. *Journal of Financial Economics, 10*(4), 407–432.
Corbet, S., & Katsiampa, P. (2020). Asymmetric mean reversion of bitcoin price returns. *International Review of Financial Analysis, 71*, Article 101267.
Corbet, S., Larkin, C., Lucey, B., Meegan, A., & Yarovaya, L. (2019). Cryptocurrency reaction to FOMC announcements: Evidence of heterogeneity based on blockchain stack position. *Journal of Financial Stability, 46*, Article 100706.
Corbet, S., Lucey, B., & Yarovaya, L. (2018). Datestamping the bitcoin and Ethereum bubbles. *Finance Research Letters, 26*, 81–88.
Cross, J. L., Hou, C., & Trinh, K. (2021). Returns, volatility and the cryptocurrency bubble of 2017–18. *Economic Modelling, 104*, Article 105643.
Da Gama Silva, P. V. J., Klotzle, M. C., Pinto, A. C. F., & Gomes, L. L. (2019). Herding behavior and contagion in the cryptocurrency market. *Journal of Behavioral and Experimental Finance, 22*, 41–50.
French, K. R., Schwert, G. W., & Stambaugh, R. F. (1987). Expected stock returns and volatility. *Journal of Financial Economics, 19*(1), 3–29.
Gkillas, K., Longin, F., & Vardas, G. (2022). Cryptocurrency contagion: Evidence from jump spillovers. *Finance Research Letters, 43*, Article 102184.
Grinsted, A., Moore, J. C., & Jevrejeva, S. (2004). Application of the cross wavelet transform and wavelet coherence to geophysical time series. *Nonlinear Processes in Geophysics, 11*(5/6), 561–566.
Kahneman, D., & Tversky, A. (1979). On the interpretation of intuitive probability: A reply to Jonathan Cohen. *Cognition, 7*(4), 409–411.
Kakinaka, S., & Umeno, K. (2022). Asymmetric volatility dynamics in cryptocurrency markets on multi-time scales. *Research in International Business and Finance, 62*, Article 101754.
Karim, M. M., Ali, M. H., Yarovaya, L., Uddin, M. H., & Hammoudeh, S. (2023). Return-volatility relationships in cryptocurrency markets: Evidence from asymmetric quantiles and non-linear ARDL approach. *International Review of Financial Analysis, 90*, Article 102894.
Karim, M. M., Kawsar, N. H., Ariff, M., & Masih, M. (2022). Does implied volatility (or fear index) affect Islamic stock returns and conventional stock returns differently? Wavelet-based granger-causality, asymmetric quantile regression and NARDL approaches. *Journal of International Financial Markets Institutions and Money, 77*, Article 101532.
Karim, M. M., & Masih, M. (2019). Do the Islamic stock market returns respond differently to the realized and implied volatility of oil prices? Evidence from the time–frequency analysis. *Emerging Markets Finance and Trade*, 1–16.
Karim, M. M., & Masih, M. (2021). Do the Islamic stock market returns respond differently to the realized and implied volatility of oil prices? Evidence from the time–frequency analysis. *Emerging Markets Finance and Trade, 57*(9), 2616–2631.
Katsiampa, P. (2017). Volatility estimation for bitcoin: A comparison of GARCH models. *Economics Letters, 158*, 3–6. https://doi.org/10.1016/j.econlet.2017.06.023
Katsiampa, P., Yarovaya, L., & Zieba, D. (2022). High-frequency connectedness between bitcoin and other top-traded crypto assets during the COVID-19 crisis. *Journal of International Financial Markets, Insitutions & Money, 79*, Article 101578.
Koenker, R. (2005). *Quantile Regression, no. 9780521845731 in Cambridge Books*.
Koenker, R., & Bassett, G., Jr. (1978). Regression quantiles. *Econometrica: Journal of the Econometric Society*, 33–50.
Koenker, R., & Hallock, K. F. (2001). Quantile regression. *Journal of Economic Perspectives, 15*(4), 143–156.
Lahiani, A., Jeribi, A., & Jlassi, N. B. (2021). Nonlinear tail dependence in cryptocurrency-stock market returns: The role of bitcoin futures. *Research in International Business and Finance, 56*, Article 101351. https://doi.org/10.1016/j.ribaf.2020.101351
Leirvik, T. (2022). Cryptocurrency returns and the volatility of liquidity. *Finance Research Letters, 44*, Article 102031.
Li, K. (2020). Does information asymmetry impede market efficiency? Evidence from analyst coverage. *Journal of Banking & Finance, 118*, Article 105856.
Nadarajah, S., & Chu, J. (2017). On the inefficiency of bitcoin. *Economics Letters, 150*, 6–9.
Naeem, M. A., Karim, S., Abrar, A., Yarovaya, L., & Shah, A. A. (2023). Non-linear relationship between oil and cryptocurrencies: Evidence from returns and shocks. *International Review of Financial Analysis, 89*.
Pal, D., & Mitra, S. K. (2017). Time-frequency contained co-movement of crude oil and world food prices: A wavelet-based analysis. *Energy Economics, 62*, 230–239.
Poyser, O. (2018). Herding behavior in cryptocurrency markets. arXiv preprint. arXiv: 1806.11348. https://arxiv.org/abs/1806.11348.
Salisu, A. A., & Ogbonna, A. E. (2022). The return volatility of cryptocurrencies during the COVID-19 pandemic: Assessing the news effect. *Global Finance Journal, 54*, Article 100641.
Selgin, G. (2015). Synthetic commodity money. *Journal of Financial Stability, 17*, 92–99.
Shefrin, H. (2008). *A behavioral approach to asset pricing*. Amsterdam, Netherlands: Elsevier.
Tiwari, A. K., Jana, R. K., Das, D., & Roubaud, D. (2018). Informational efficiency of bitcoin—An extension. *Economics Letters, 163*, 106–109.
Torrence, C., & Webster, P. J. (1999). Interdecadal changes in the ENSO–monsoon system. *Journal of Climate, 12*(8), 2679–2690.
Trucíos, C. (2019). Forecasting bitcoin risk measures: A robust approach. *International Journal of Forecasting, 35*(3), 836–847.
Tversky, A., & Kahneman, D. (1974). Judgment under uncertainty: Heuristics and biases: Biases in judgments reveal some heuristics of thinking under uncertainty. *science, 185*(4157), 1124–1131.
Urquhart, A. (2016). The inefficiency of bitcoin. *Economics Letters, 148*, 80–82.
Voev, V., & Lunde, A. (2007). Integrated covariance estimation using high-frequency data in the presence of noise. *Journal of Financial Econometrics, 5*(1), 68–104.
Wan Jamarul Imran, W. A., Yahya, M. H., Ali, M. H., & Abdul Basir, M. A. Q. (2021). How information asymmetry and cybercriminal risk affect volatility and return of cryptocurrencies. *Journal of Academia, 9*, 121–130.
Wang, J., & Ngene, G. M. (2020). Does bitcoin still own the dominant power? An intradayanalysis. *International Review of Financial Analysis, 71*(101551), 93.
Wang, X., Liu, J., & Xie, Q. (2024). Quantile frequency connectedness between energy tokens, crypto market, and renewable energy stock markets. *Heliyon, 10*(3).
Wang, Y., Luvey, B. M., Vigne, S. A., & Yarovaya, L. (2022). The effects of central Bank digital currencies news on financial markets. *Technological Forecasting and Social Change, 180*, Article 121715.
Wei, W. C. (2018). Liquidity and market efficiency in cryptocurrencies. *Economics Letters, 168*, 21–24.
Whaley, R. E. (2000). The investor fear gauge. *The Journal of Portfolio Management, 26*(3), 12–17.
Yarovaya, L., Matkovskyy, R., & Jalan, A. (2020). *The effects of a "Black Swan" event (COVID-19) on herding behavior in cryptocurrency markets: Evidence from cryptocurrency USD, EUR, JPY and KRW markets. EUR, JPY and KRW markets (April 27, 2020)*.
Yarovaya, L., & Zieba, D. (2022). Intraday volume-return nexus in cryptocurrency markets: Novel evidence from cryptocurrency classification. *Research in International Business and Finance, 90*, 1015.
Yu, J. H., Kang, J., & Park, S. (2019). Information availability and return volatility in the bitcoin market: analyzing differences of user opinion and interest. *Information Processing & Management, 56*(3), 721–732.
Zhang, Z., & Zhao, R. (2023). Good volatility, bad volatility, and the cross section of cryptocurrency returns. *International Review of Financial Analysis, 89*.